Acta Mech 233, 2173–2199 (2022)
https://doi.org/10.1007/s00707-022-03209-3

ORIGINAL PAPER

Xin Feng · Zhiming Hu · Han Zhang · Liangliang Zhang · Yang Gao

Semi-analytical solutions for functionally graded cubic quasicrystal laminates with mixed boundary conditions

Received: 26 October 2021 / Revised: 29 March 2022 / Accepted: 11 April 2022 / Published online: 17 May 2022

Abstract Tremendous attention of researchers has been attracted by the unusual properties of quasicrystals. In this paper, the static solution of functionally gradient multilayered cubic quasicrystal plates on an elastic foundation with mixed boundary conditions is presented based on the linear elastic theory of quasicrystals. The quasicrystal material properties are assumed to have an exponent-law variation along the thickness direction. The elastic foundation is taken as the Winkler–Pasternak model, which is utilized to simulate the interaction between the plate and the elastic medium. The multilayered quasicrystal structures with two opposite edges simply supported and simply/clamped/free supported boundary conditions at other edges are considered. The semi-analytical method, which makes use of the state-space method in the z-direction, the one-dimensional differential quadrature method in the x-direction, and the series solution in the y-direction, is adopted to convert the system of governing partial differential equations into the ordinary one. From the propagator matrix, the static solution can be derived by imposing the boundary conditions on the top and bottom surfaces of the multilayered plates. Finally, typical numerical examples are presented to verify the effectiveness of this method and illustrate the influence of different boundary conditions, stacking sequence, foundation parameters, and functionally gradient exponential factors on the phonon and phason variables.

1 Introduction

Quasicrystals (QCs) are new type of composite materials, and the ordered and quasi-periodic atomic arrangement in QCs enables them to exhibit some complex structures and special properties in theoretical analysis and experiments, such as high hardness, high toughness, high abrasion resistance, high resistivity, low friction coefficient, and low thermal conductivity [1, 2]. These attractive properties in QCs enable them to have many potential applications [3, 4], such as the solar thin film, thermoelectric converters, and structural enhancement phase of composites. In particular, multilayered structures containing QC with excellent electrical and mechanical properties would be gradually used in the new generation of information technology and semiconductor fields, such as micro-electromechanical systems and nanoelectromechanical systems [5]. Therefore, it is tremendously significant to investigate the multilayered QC plate actuators driven by electrostatic or piezoelectric actuators, which can be helpful for analyzing and designing electromechanical systems. However, the

Z. Hu · L. Zhang (✉) · Y. Gao (✉)
College of Science, China Agricultural University, Beijing 100083, People's Republic of China
e-mail: llzhang@cau.edu.cn

Y. Gao
e-mail: gaoyangg@gmail.com

X. Feng
College of Engineering, China Agricultural University, Beijing 100083, People's Republic of China

H. Zhang
Chinese Academy of Sciences, Beijing 100190, People's Republic of China

mismatch of the material coefficients between the driven diaphragms may initiate the disadvantages of the debonding, micro-cracks, and delamination.

Functionally graded materials (FGMs) are inhomogeneous composite materials, and the mechanical properties vary continuously over a macroscale geometrical dimension [6]. Different from the conventional laminated materials, FGMs do not possess discernible internal phase boundaries, which directly avoids slight stress concentration caused by kinds of external loads [7]. Thus, FGMs can be used to improve the structural performance of multilayer plates. The structure of Al-Cu-Fe alloys solidified by chill casting was investigated to reveal the peritectic reactions underlying the metastable to stable QC structure transformation [8]. After that, a double-layer FG structure reinforced with QC approximant phases has been prepared to alternate the gradient properties parts [9]. Similarly, Ferreira et al. [10] presented a new FG material to improve the wear resistance at high temperatures. In order to fully exploit the merits of QC materials, the researchers also performed some theoretical analyses of the FG QC structures. Based on the nonlocal elasticity theory, Zhang et al. [11, 12] derived the exact solution for a simply supported FG one-dimensional (1D) hexagonal piezoelectric QC nanoplate under surface mechanical loadings. According to the state-space method and propagator matrix method, Huang et al. [13] obtained the static solution of the FG multilayered 1D piezoelectric QC simply-supported plate subjected to mechanical and electrical load on its top surface. Li et al. [14] presented the thermo-elastic analysis of simply supported FG two-dimensional (2D) QC plates under a thermal load by using the pseudo-Stroh formalism and propagator matrix method. After that, Li et al. [15] investigated the static deformation of the FGs layered 2D piezoelectric QC simply supported plate subjected to an electric potential load by using the same methods. However, in the studies mentioned above, the FG QC laminates were analyzed with simply supported boundary conditions. In addition, to the best of the authors' knowledge, no mechanical analysis of FG three-dimensional (3D) cubic QC with mixed boundary conditions has been performed so far.

Although the pseudo-Stroh formalism and state-space method can be used to derive the exact solution for the FG QC laminates with simply supported boundary conditions by using the general displacement and stress solutions, the plates with the clamped-supported and mixed boundary conditions cannot be solved. However, some semi-analytical numerical methods [16–18] can be used to derive the solutions of the static response and free vibration for plates with arbitrary boundary conditions. The differential quadrature method (DQM) has been approved as highly efficient for the rapid solution of differential equations governing boundary/initial problems during the past decades [19, 20]. The basic idea of DQM is to approximate an unknown function and its partial derivatives with respect to a spatial variable at any discrete point are converted into linear weighted sums. Thus, it is convenient for this method to deal with arbitrary supporting conditions and reduce the dimension of the final governing equations. Lü et al. [18] analyzed the free vibration of laminated plates under mixed boundary conditions by using the DQM. Zhou et al. also utilized the same method to analyze the dynamic response of piezoelectric plates with arbitrary boundary conditions[21]and the cylindrical bending for piezoelectric laminates with imperfect interfaces [22].

Meanwhile, foundation models have been widely adopted by many researchers to simulate the interaction between elastic media and plates in engineering fields, such as raft foundations, airport runways, storage tanks, and most civil engineering constructions [23, 24]. The basic idea of foundation models is an interface boundary condition, and it can be treated by using DQM. For example, Yas and Jodaei [25] derived the dynamic behavior of the annular plates on elastic foundations by utilizing the DQM and analyzed the influences of the material property graded index, circumferential wave number, foundation parameters, and thickness on the natural frequency of the annular plate with different boundary conditions. At the same time, Yas and Moloudi [26] presented the solution of the free vibration for a piezoelectric ring plate with the same method and studied the influence of the Winkler elastic foundation constant on the natural frequency of the plate under different boundary conditions. After that, based on the 3D elasticity theory, Malekzadeh [27] investigated an accurate solution procedure for the free vibration analysis of FG thick plates on a two-parameter elastic foundation.

In this paper, the state-space-based differential quadrature method (SS-DQM) is developed to investigate the static response problems for FG multilayered 3D cubic QC thick plates with mixed boundary conditions on a two-parameter elastic foundation. Based on the QC linear elasticity theory, FG QC plates with two opposite edges simply supported and simply/clamped/free supported boundary conditions at the other edges are considered. The DQM and series solution are utilized to translate the partial differential equation into an ordinary differential equation. Making use of the boundary conditions of the top and bottom surfaces of the laminate and foundation model, the solutions can be derived from the global propagator matrix. Finally, the numerical examples are presented to verify the accuracy of SS-DQM and illustrate the influence of different boundary conditions, stacking sequence, foundation parameters, and FG exponential factor on the phonon

and phason variables. The numerical results indicate that the hybrid method is an effective tool to predict the accurate behavior of FG QC composite laminated structures with mixed boundary conditions. Meanwhile, the numerical results can also serve as a reference for verifying existing or future FG QC plate theories.

2 Mathematical formulations

Consider an M-layer FG 3D cubic QC rectangular plate with the total thickness H in the vertical direction and horizontal dimensions $x \times y = L_x \times L_y$, as shown in Fig. 1. The atomic arrangement of the 3D cubic QC is quasi-periodic in the x, y, and z directions. The relationship between the global Cartesian coordinate system and the local material coordinate system of the plates is assumed to be $(x, y, z) = (x_1, x_2, x_3)$. The pth layer with thickness $h_p = z_p - z_{p-1}$ ($p = 1, 2, 3, \ldots, M$) is bounded by the lower interface at $z = z_{p-1}$ and the upper interface at $z = z_p$. It follows that the bottom and top surfaces of the laminate are $z_0 = 0$ and $z_M = H$, respectively.

2.1 Basic equations

In this part, the material local coordinate system (x_1, x_2, x_3) is utilized to describe the basic equations of 3D cubic QC material. According to the QC linear elastic theory, the stress–strain relationship of the 3D cubic QC can be written as [28, 29]

$$
\begin{aligned}
\sigma_{11} &= C_{11}\varepsilon_{11} + C_{12}\varepsilon_{22} + C_{12}\varepsilon_{33} + R_1 w_{11} + R_2 w_{22} + R_2 w_{33},\\
\sigma_{22} &= C_{12}\varepsilon_{11} + C_{11}\varepsilon_{22} + C_{12}\varepsilon_{33} + R_2 w_{11} + R_1 w_{22} + R_2 w_{33},\\
\sigma_{33} &= C_{12}\varepsilon_{11} + C_{12}\varepsilon_{22} + C_{11}\varepsilon_{33} + R_2 w_{11} + R_2 w_{22} + R_1 w_{33},\\
\sigma_{23} &= \sigma_{32} = 2C_{44}\varepsilon_{23} + 2R_3 w_{23},\\
\sigma_{13} &= \sigma_{31} = 2C_{44}\varepsilon_{31} + 2R_3 w_{31},\\
\sigma_{12} &= \sigma_{21} = 2C_{44}\varepsilon_{12} + 2R_3 w_{12},\\
H_{11} &= R_1\varepsilon_{11} + R_2\varepsilon_{22} + R_2\varepsilon_{33} + K_{11} w_{11} + K_{12} w_{22} + K_{12} w_{33},\\
H_{22} &= R_2\varepsilon_{11} + R_1\varepsilon_{22} + R_2\varepsilon_{33} + K_{12} w_{11} + K_{11} w_{22} + K_{12} w_{33},\\
H_{33} &= R_2\varepsilon_{11} + R_2\varepsilon_{22} + R_1\varepsilon_{33} + K_{12} w_{11} + K_{12} w_{22} + K_{11} w_{33},\\
H_{23} &= H_{32} = 2R_3\varepsilon_{23} + 2K_{44} w_{23},\\
H_{13} &= H_{31} = 2R_3\varepsilon_{31} + 2K_{44} w_{31},\\
H_{12} &= H_{21} = 2R_3\varepsilon_{12} + 2K_{44} w_{12},
\end{aligned}
\tag{1}
$$

where C_{mn} ($m, n = 1, 2, 4$), K_{mn}, and R_i ($i = 1, 2, 3$) represent the phonon, phason, and phonon–phason coupling elastic coefficients, respectively; the phonon stresses and phason stresses are denoted by σ_{ij} ($j = 1, 2, 3$) and H_{ij}, respectively; ε_{ij} and w_{ij} are defined as the phonon and phason strains, respectively.

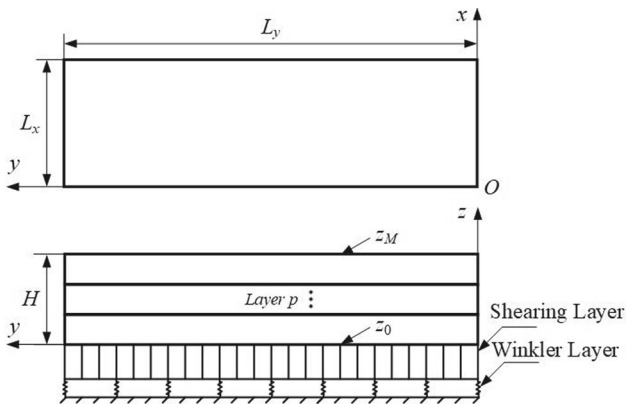

Fig. 1 An M-layered FG 3D cubic QC plate

The strain–displacement relations for 3D cubic QCs [30] are given by

$$\begin{aligned}
&\varepsilon_{11}=\frac{\partial u_1}{\partial x_1},\quad \varepsilon_{22}=\frac{\partial u_2}{\partial x_2},\quad \varepsilon_{33}=\frac{\partial u_3}{\partial x_3},\quad \varepsilon_{12}=\varepsilon_{21}=\frac{1}{2}\left(\frac{\partial u_1}{\partial x_2}+\frac{\partial u_2}{\partial x_1}\right),\\
&\varepsilon_{13}=\varepsilon_{31}=\frac{1}{2}\left(\frac{\partial u_1}{\partial x_3}+\frac{\partial u_3}{\partial x_1}\right),\quad \varepsilon_{23}=\varepsilon_{32}=\frac{1}{2}\left(\frac{\partial u_2}{\partial x_3}+\frac{\partial u_3}{\partial x_2}\right),\\
&w_{11}=\frac{\partial w_1}{\partial x_1},\quad w_{22}=\frac{\partial w_2}{\partial x_2},\quad w_{33}=\frac{\partial w_3}{\partial x_3},\quad w_{12}=w_{21}=\frac{1}{2}\left(\frac{\partial w_1}{\partial x_2}+\frac{\partial w_2}{\partial x_1}\right),\\
&w_{13}=w_{31}=\frac{1}{2}\left(\frac{\partial w_1}{\partial x_3}+\frac{\partial w_3}{\partial x_1}\right),\quad w_{23}=w_{32}=\frac{1}{2}\left(\frac{\partial w_2}{\partial x_3}+\frac{\partial w_3}{\partial x_2}\right),
\end{aligned}\tag{2}$$

where u_i and w_i represent the phonon and phason displacements, respectively.

In the absence of body forces, the static equilibrium equations [28] are governed by

$$\begin{aligned}
&\frac{\partial\sigma_{11}}{\partial x_1}+\frac{\partial\sigma_{12}}{\partial x_2}+\frac{\partial\sigma_{13}}{\partial x_3}=0,\quad \frac{\partial\sigma_{21}}{\partial x_1}+\frac{\partial\sigma_{22}}{\partial x_2}+\frac{\partial\sigma_{23}}{\partial x_3}=0,\quad \frac{\partial\sigma_{31}}{\partial x_1}+\frac{\partial\sigma_{32}}{\partial x_2}+\frac{\partial\sigma_{33}}{\partial x_3}=0,\\
&\frac{\partial H_{11}}{\partial x_1}+\frac{\partial H_{12}}{\partial x_2}+\frac{\partial H_{13}}{\partial x_3}=0,\quad \frac{\partial H_{21}}{\partial x_1}+\frac{\partial H_{22}}{\partial x_2}+\frac{\partial H_{23}}{\partial x_3}=0,\quad \frac{\partial H_{31}}{\partial x_1}+\frac{\partial H_{32}}{\partial x_2}+\frac{\partial H_{33}}{\partial x_3}=0.
\end{aligned}\tag{3}$$

It is assumed that the material properties of FG QC are exponentially distributed along the x_3-direction. So, the material constants in Eq. (1) can be rewritten as

$$F(x_3)=F^0e^{\eta x_3},\tag{4}$$

where η is the exponential factor characterizing the degree of the material gradient in the x_3-direction; F^0 indicates the initial values of material constants in Eq. (1). It follows that $\eta=0$ represents the homogeneous QC material case.

2.2 General solution

The Cartesian coordinate system (x, y, z) is utilized to describe the static response of QC laminates. The state-space approach is based on the mixed equations of the solid mechanics in which $u_x, u_y, w_x, w_y, \sigma_{zz}, H_{zz}, \sigma_{xz}, \sigma_{yz}, H_{xz}, H_{yz}, u_z, w_z$ are taken as basic unknowns. Eliminating $\sigma_{xx}, \sigma_{yy}, \sigma_{xy}, H_{xx}, H_{yy}, H_{zz}$ from Eqs. (1)–(3) and following the process of the state-space method, the state equation can be written as

$$\frac{\partial}{\partial z}\boldsymbol{\theta}=\mathbf{D}\grave{},\tag{5}$$

where $\boldsymbol{\theta}$ is the basic unknown vector and is also called the state vector. The coefficient matrix $\mathbf{D}$ is

$$\mathbf{D}=\begin{bmatrix}\mathbf{0} & \mathbf{D}_1\\ \mathbf{D}_2 & \mathbf{0}\end{bmatrix}.\tag{6}$$

The submatrices $\mathbf{D}_1$ and $\mathbf{D}_2$ in Eq. (6) are

$$\mathbf{D}_1=\begin{bmatrix}
\frac{a_4}{a_1} & 0 & -\frac{a_3}{a_1} & 0 & \left(\frac{a_3^2-a_2a_4}{a_1}\right)\frac{\partial}{\partial x} & 0\\
0 & \frac{a_4}{a_1} & 0 & -\frac{a_3}{a_1} & \left(\frac{a_3^2-a_2a_4}{a_1}\right)\frac{\partial}{\partial y} & 0\\
-\frac{a_3}{a_1} & 0 & \frac{a_2}{a_1} & 0 & 0 & \left(\frac{a_3^2-a_2a_4}{a_1}\right)\frac{\partial}{\partial x}\\
0 & -\frac{a_3}{a_1} & 0 & \frac{a_2}{a_1} & 0 & \left(\frac{a_3^2-a_2a_4}{a_1}\right)\frac{\partial}{\partial y}\\
-\frac{\partial}{\partial x} & -\frac{\partial}{\partial y} & 0 & 0 & 0 & 0\\
0 & 0 & -\frac{\partial}{\partial x} & -\frac{\partial}{\partial y} & 0 & 0
\end{bmatrix},$$

$$\mathbf{D}_2 = \begin{bmatrix} b_1 & a_9\frac{\partial^2}{\partial x\partial y} & a_{11}\frac{\partial^2}{\partial x^2} - a_3\frac{\partial^2}{\partial y^2} & a_{12}\frac{\partial^2}{\partial x\partial y} & \frac{a_{13}}{a_6}\frac{\partial}{\partial x} & \frac{a_{14}}{a_6}\frac{\partial}{\partial x} \\ & -a_2\frac{\partial^2}{\partial x^2} + a_8\frac{\partial^2}{\partial y^2} & a_{12}\frac{\partial^2}{\partial x\partial y} & -a_3\frac{\partial^2}{\partial x^2} + a_{11}\frac{\partial^2}{\partial y^2} & \frac{a_{13}}{a_6}\frac{\partial}{\partial y} & \frac{a_{14}}{a_6}\frac{\partial}{\partial y} \\ & & b_2 & a_{17}\frac{\partial^2}{\partial x\partial y} & \frac{a_{18}}{a_6}\frac{\partial}{\partial x} & \frac{a_{19}}{a_6}\frac{\partial}{\partial x} \\ \mathbf{Sym} & & & -a_4\frac{\partial^2}{\partial x^2} + a_{16}\frac{\partial^2}{\partial y^2} & \frac{a_{18}}{a_6}\frac{\partial}{\partial y} & \frac{a_{19}}{a_6}\frac{\partial}{\partial y} \\ & & & & a_{20} & a_{21} \\ & & & & & a_5 \end{bmatrix} \tag{7}$$

where the symmetric part of the matrix is expressed as **Sym**. The coefficients in Eq. (7) and the following equations can be found in Eq. (A.1) of "Appendix A".

The stress components eliminated in Eq. (5) can be written as

$$\begin{aligned}
\sigma_{xx} &= -a_8\frac{\partial u_x}{\partial x} - (a_9 + a_2)\frac{\partial u_y}{\partial y} - a_{11}\frac{\partial w_x}{\partial x} - (a_{12} + a_3)\frac{\partial w_y}{\partial y} - \frac{a_{13}}{a_6}\sigma_{zz} - \frac{a_{14}}{a_6}H_{zz}, \\
\sigma_{yy} &= -(a_9 + a_2)\frac{\partial u_x}{\partial x} - a_8\frac{\partial u_y}{\partial y} - (a_{12} + a_3)\frac{\partial w_x}{\partial x} - a_{11}\frac{\partial w_y}{\partial y} - \frac{a_{13}}{a_6}\sigma_{zz} - \frac{a_{14}}{a_6}H_{zz}, \\
\sigma_{xy} &= a_2\frac{\partial u_x}{\partial y} + a_2\frac{\partial u_y}{\partial x} + a_3\frac{\partial w_x}{\partial y} + a_3\frac{\partial w_y}{\partial x}, \\
H_{xx} &= a_1\frac{\partial u_x}{\partial x} - (a_{12} + a_3)\frac{\partial u_y}{\partial y} - a_{16}\frac{\partial w_x}{\partial x} - (a_{17} + a_4)\frac{\partial w_y}{\partial y} - \frac{a_{18}}{a_6}\sigma_{zz} - \frac{a_{19}}{a_6}H_{zz}, \\
H_{yy} &= a_1\frac{\partial u_x}{\partial x} - (a_{12} + a_3)\frac{\partial u_y}{\partial y} - a_{16}\frac{\partial w_x}{\partial x} - (a_{17} + a_4)\frac{\partial w_y}{\partial y} - \frac{a_{18}}{a_6}\sigma_{zz} - \frac{a_{19}}{a_6}H_{zz}, \\
H_{xy} &= a_3\frac{\partial u_x}{\partial y} + a_3\frac{\partial u_y}{\partial x} + a_4\frac{\partial w_x}{\partial y} + a_4\frac{\partial w_y}{\partial x}.
\end{aligned} \tag{8}$$

The boundary conditions in the y-direction for the QC laminates can be written as follows:

$$y = 0, \quad L_y : u_x = u_z = w_x = w_z = \sigma_{yy} = H_{yy} = 0. \tag{9}$$

The displacement and stress variables, which satisfy these boundary conditions [29, 31], can be written as

$$\begin{bmatrix} u_x(x,y,z) \\ u_y(x,y,z) \\ w_x(x,y,z) \\ w_y(x,y,z) \\ \sigma_{zz}(x,y,z) \\ H_{zz}(x,y,z) \end{bmatrix} = \sum_{l=1}^{\infty} \begin{bmatrix} \tilde{u}_x(x,z)\sin(qy) \\ \tilde{u}_y(x,z)\cos(qy) \\ \tilde{w}_x(x,z)\sin(qy) \\ \tilde{w}_y(x,z)\cos(qy) \\ \tilde{\sigma}_{zz}(x,z)\sin(qy) \\ \tilde{H}_{zz}(x,z)\sin(qy) \end{bmatrix}, \begin{bmatrix} \sigma_{xz}(x,y,z) \\ \sigma_{yz}(x,y,z) \\ H_{xz}(x,y,z) \\ H_{yz}(x,y,z) \\ u_z(x,y,z) \\ w_z(x,y,z) \end{bmatrix} = \sum_{l=1}^{\infty} \begin{bmatrix} \tilde{\sigma}_{xz}(x,z)\sin(qy) \\ \tilde{\sigma}_{yz}(x,z)\cos(qy) \\ \tilde{H}_{xz}(x,z)\sin(qy) \\ \tilde{H}_{yz}(x,z)\cos(qy) \\ \tilde{u}_z(x,z)\sin(qy) \\ \tilde{w}_z(x,z)\sin(qy) \end{bmatrix}, \tag{10}$$

where $\tilde{u}_x, \tilde{u}_y, \tilde{w}_x, \tilde{w}_y, \tilde{\sigma}_{zz}, \tilde{H}_{zz}, \tilde{\sigma}_{xz}, \tilde{\sigma}_{yz}, \tilde{H}_{xz}, \tilde{H}_{yz}, \tilde{u}_z, \tilde{w}_z$ are the unknown functions; $q = l\pi/L_y$ with l being the number of superposition.

Incorporating Eq. (5) with Eq. (10) yields

$$\frac{\partial}{\partial z}\tilde{\boldsymbol{\theta}} = \tilde{\mathbf{D}}\tilde{\boldsymbol{\theta}}, \tag{11}$$

where $\tilde{}(x,z) = \left[\tilde{u}_x, \tilde{u}_y, \tilde{w}_x, \tilde{w}_y, \tilde{\sigma}_{zz}, \tilde{H}_{zz}, \tilde{\sigma}_{xz}, \tilde{\sigma}_{yz}, \tilde{H}_{xz}, \tilde{H}_{yz}, \tilde{u}_z, \tilde{w}_z\right]^{\mathrm{T}}$, in which the superscript 'T' denotes transpose; $\tilde{\mathbf{D}}$ is the coefficient matrix.

Substituting Eq. (10) into Eq. (8), the equations can be rewritten as

$$\begin{aligned}
\tilde{\sigma}_{xx} &= -a_8\frac{\partial \tilde{u}_x}{\partial x} + (a_9 + a_2)q\tilde{u}_y - a_{11}\frac{\partial \tilde{w}_x}{\partial x} + (a_{12} + a_3)q\tilde{w}_y - \frac{a_{13}}{a_6}\tilde{\sigma}_{zz} - \frac{a_{14}}{a_6}\tilde{H}_{zz}, \\
\tilde{\sigma}_{yy} &= -(a_9 + a_2)\frac{\partial \tilde{u}_x}{\partial x} + a_8 q\tilde{u}_y - (a_{12} + a_3)\frac{\partial \tilde{w}_x}{\partial x} + a_{11}q\tilde{w}_y - \frac{a_{13}}{a_6}\tilde{\sigma}_{zz} - \frac{a_{14}}{a_6}\tilde{H}_{zz}, \\
\tilde{\sigma}_{xy} &= a_2 q\tilde{u}_x + a_2\frac{\partial \tilde{u}_y}{\partial x} + a_3 q\tilde{w}_x + a_3\frac{\partial \tilde{w}_y}{\partial x},
\end{aligned}$$

$$\tilde{H}_{xx} = a_1\frac{\partial \tilde{u}_x}{\partial x} + (a_{12}+a_3)q\tilde{u}_y - a_{16}\frac{\partial \tilde{w}_x}{\partial x} + (a_{17}+a_4)q\tilde{w}_y - \frac{a_{18}}{a_6}\tilde{\sigma}_{zz} - \frac{a_{19}}{a_6}\tilde{H}_{zz},$$
$$\tilde{H}_{yy} = a_1\frac{\partial \tilde{u}_x}{\partial x} + (a_{12}+a_3)q\tilde{u}_y - a_{16}\frac{\partial \tilde{w}_x}{\partial x} + (a_{17}+a_4)q\tilde{w}_y - \frac{a_{18}}{a_6}\tilde{\sigma}_{zz} - \frac{a_{19}}{a_6}\tilde{H}_{zz},$$
$$\tilde{H}_{xy} = a_3 q\tilde{u}_x + a_3\frac{\partial \tilde{u}_y}{\partial x} + a_4 q\tilde{w}_x + a_4\frac{\partial \tilde{w}_y}{\partial x}. \tag{12}$$

However, the solutions of the same form in Eq. (10) cannot satisfy the clamped/free-supported boundary conditions in the x-direction. Therefore, it is difficult to derive an exact solution for the FG QC plate. Here, the DQM is used to deal with this problem. And the basic idea of this method is to approximate an unknown function, and its partial derivatives with respect to a spatial variable at any discrete point are converted into linear weighted sums. So the partial differential equation in Eq. (11) can be translated into an ordinary differential equation. The nth-order derivative of an unknown function $f(x)$ at discrete point r can be written as

$$\left.\frac{\partial^n f(x)}{\partial x^n}\right|_{x=x_r} = \sum_{k=1}^{N} X_{rk}^{(n)} f(x_k) \quad (r = 1, 2, \ldots, N), \tag{13}$$

where N is the number of sampling points; $f(x_k)$ is the function value at the discrete point r; $X_{rk}^{(n)}$ is the nth-order weighting coefficient matrix.

Five kinds of discrete patterns are taken in Refs. [32, 33]. Here, the Chebyshev–Gauss–Lobatto grid space model in the in-plane discrete direction is adopted, as follows:

$$x_r = \frac{L_x}{2}\left[1 - \cos\left(\frac{r-1}{N-1}\pi\right)\right], \quad r = 1, 2, 3, \ldots N, \tag{14}$$

Thus, the mixed boundary conditions in the x-direction for the FG QC plate can be written as

$$\text{Simply supported (S)}: \quad \tilde{u}_{yd} = \tilde{u}_{zd} = \tilde{w}_{yd} = \tilde{w}_{zd} = \tilde{\sigma}_{xxd} = \tilde{H}_{xxd} = 0, \tag{15}$$

$$\text{Clamped (C)}: \quad \tilde{u}_{xd} = \tilde{u}_{yd} = \tilde{u}_{zd} = \tilde{w}_{xd} = \tilde{w}_{yd} = \tilde{w}_{zd} = 0, \tag{16}$$

$$\text{Free (F)}: \quad \tilde{\sigma}_{xx} = \tilde{\sigma}_{xy} = \tilde{\sigma}_{xz} = \tilde{H}_{xx} = \tilde{H}_{xy} = \tilde{H}_{xz} = 0, \tag{17}$$

where $d = 1$ and N; 'S' indicates the simply-supported boundary condition, 'C' is the clamped-supported boundary condition, and 'F' is the free-supported boundary condition. For example, 'CSCS' denotes a plate with the clamped-supported boundary condition at $x = 0$ and $x = L_x$, and others are simply supported at $y = 0$ and $y = L_y$, respectively.

Using DQM to the state space Eq. (11), the new state equations at any discrete points can be rewritten as

$$\frac{\mathrm{d}\tilde{u}_{xr}}{\mathrm{d}z} = \frac{a_4}{a_1}\tilde{\sigma}_{xzr} - \frac{a_3}{a_1}\tilde{H}_{xzr} + \left(\frac{a_3^2 - a_2a_4}{a_1}\right)\sum_{k=1}^{N} X_{rk}^{(1)}\tilde{u}_{zk},$$
$$\frac{\mathrm{d}\tilde{u}_{yr}}{\mathrm{d}z} = \frac{a_4}{a_1}\tilde{\sigma}_{yzr} + \frac{a_4}{a_1}\tilde{H}_{yzr} + \left(\frac{a_3^2 - a_2a_4}{a_1}\right)q\tilde{u}_{zr},$$
$$\frac{\mathrm{d}\tilde{w}_{xr}}{\mathrm{d}z} = -\frac{a_3}{a_1}\tilde{\sigma}_{xzr} + \frac{a_2}{a_1}\tilde{H}_{xzr} + \left(\frac{a_3^2 - a_2a_4}{a_1}\right)\sum_{k=1}^{N} X_{rk}^{(1)}\tilde{w}_{zk},$$
$$\frac{\mathrm{d}\tilde{w}_{yr}}{\mathrm{d}z} = -\frac{a_3}{a_1}\tilde{\sigma}_{yzr} + \frac{a_2}{a_1}\tilde{H}_{yzr} + \left(\frac{a_3^2 - a_2a_4}{a_1}\right)q\tilde{w}_{zr},$$
$$\frac{\mathrm{d}\tilde{\sigma}_{zzr}}{\mathrm{d}z} = -\sum_{k=1}^{N} X_{rk}^{(1)}\tilde{\sigma}_{xzr} + q\tilde{\sigma}_{yzr},$$
$$\frac{\mathrm{d}\tilde{H}_{zzr}}{\mathrm{d}z} = -\sum_{k=1}^{N} X_{rk}^{(1)}\tilde{H}_{xzr} + q\tilde{H}_{yzr},$$

$$
\begin{aligned}
\frac{\mathrm{d}\tilde{\sigma}_{xzr}}{\mathrm{d}z} &= a_8\sum_{k=1}^{N}X_{rk}^{(2)}\tilde{u}_{xk}+a_2q^2\tilde{u}_{xr}-a_9q\sum_{k=1}^{N}X_{rk}^{(1)}\tilde{u}_{yk}+a_{11}\sum_{k=1}^{N}X_{rk}^{(2)}\tilde{w}_{xk}+a_3q^2\tilde{w}_{xr}\\
&\quad -a_{12}q\sum_{k=1}^{N}X_{rk}^{(1)}\tilde{w}_{yk}+\frac{a_{13}}{a_6}\sum_{k=1}^{N}X_{rk}^{(1)}\tilde{\sigma}_{zzk}+\frac{a_{14}}{a_6}\sum_{k=1}^{N}X_{rk}^{(1)}\tilde{H}_{zzk},\\
\frac{\mathrm{d}\tilde{\sigma}_{yzr}}{\mathrm{d}z} &= a_9q\sum_{k=1}^{N}X_{rk}^{(1)}\tilde{u}_{xk}-a_2\sum_{k=1}^{N}X_{rk}^{(2)}\tilde{u}_{yk}-a_8q^2\tilde{u}_{yr}+a_{12}q\sum_{k=1}^{N}X_{rk}^{(1)}\tilde{w}_{xk}\\
&\quad -a_3\sum_{k=1}^{N}X_{rk}^{(2)}\tilde{w}_{yk}-a_{11}q^2\tilde{w}_{yr}+\frac{a_{13}}{a_6}q\tilde{\sigma}_{zzr}+\frac{a_{14}}{a_6}q\tilde{H}_{zzr},\\
\frac{\mathrm{d}\tilde{H}_{xzr}}{\mathrm{d}z} &= a_{11}\sum_{k=1}^{N}X_{rk}^{(2)}\tilde{u}_{xk}+a_3q^2\tilde{u}_{xr}-a_{12}q\sum_{k=1}^{N}X_{rk}^{(1)}\tilde{u}_{yk}+a_{16}\sum_{k=1}^{N}X_{rk}^{(2)}\tilde{w}_{xk}+a_4q^2\tilde{w}_{xr}\\
&\quad -a_{17}q\sum_{k=1}^{N}X_{rk}^{(1)}\tilde{w}_{yk}+\frac{a_{18}}{a_6}\sum_{k=1}^{N}X_{rk}^{(1)}\tilde{\sigma}_{zzk}+\frac{a_{19}}{a_6}\sum_{k=1}^{N}X_{rk}^{(1)}\tilde{H}_{zzk},\\
\frac{\mathrm{d}\tilde{H}_{yzr}}{\mathrm{d}z} &= a_{12}q\sum_{k=1}^{N}X_{rk}^{(1)}\tilde{u}_{xk}-a_3\sum_{k=1}^{N}X_{rk}^{(2)}\tilde{u}_{yk}-a_{11}q^2\tilde{u}_{yr}+a_{17}q\sum_{k=1}^{N}X_{rk}^{(1)}\tilde{w}_{xk}-a_4\sum_{k=1}^{N}X_{rk}^{(2)}\tilde{w}_{yk}\\
&\quad -a_{16}q^2\tilde{w}_{yr}+\frac{a_{18}}{a_6}q\tilde{\sigma}_{zzr}+\frac{a_{19}}{a_6}q\tilde{H}_{zzr},\\
\frac{\mathrm{d}\tilde{u}_{zr}}{\mathrm{d}z} &= \frac{a_{13}}{a_6}\sum_{k=1}^{N}X_{rk}^{(1)}\tilde{u}_{xk}-\frac{a_{13}}{a_6}q\tilde{u}_{yr}+\frac{a_{18}}{a_6}\sum_{k=1}^{N}X_{rk}^{(1)}\tilde{w}_{xk}-\frac{a_{18}}{a_6}q\tilde{w}_{yr}+a_{20}\tilde{\sigma}_{zzr}+a_{21}\tilde{H}_{zzr},\\
\frac{\mathrm{d}\tilde{w}_{zr}}{\mathrm{d}z} &= \frac{a_{14}}{a_6}\sum_{k=1}^{N}X_{rk}^{(1)}\tilde{u}_{xk}-\frac{a_{14}}{a_6}q\tilde{u}_{yr}+\frac{a_{19}}{a_6}\sum_{k=1}^{N}X_{rk}^{(1)}\tilde{w}_{xk}-\frac{a_{19}}{a_6}q\tilde{w}_{yr}+a_{21}\tilde{\sigma}_{zzr}+a_5\tilde{H}_{zzr}.
\end{aligned}
\tag{18}
$$

Similarly, at the same discrete point, Eq. (12) can be rewritten as

$$
\begin{aligned}
\tilde{\sigma}_{xxr} &= -a_8\sum_{k=1}^{N}X_{rk}^{(1)}\tilde{u}_{xk}+(a_9+a_2)q\tilde{u}_{yr}-a_{11}\sum_{k=1}^{N}X_{rk}^{(1)}\tilde{w}_{xk}+(a_{12}+a_3)q\tilde{w}_{yr}-\frac{a_{13}}{a_6}\tilde{\sigma}_{zzr}-\frac{a_{14}}{a_6}\tilde{H}_{zzr},\\
\tilde{\sigma}_{yyr} &= -(a_9+a_2)\sum_{k=1}^{N}X_{rk}^{(1)}\tilde{u}_{xk}+a_8q\tilde{u}_{yr}-(a_{12}+a_3)\sum_{k=1}^{N}X_{rk}^{(1)}\tilde{w}_{xk}+a_{11}q\tilde{w}_{yr}-\frac{a_{13}}{a_6}\tilde{\sigma}_{zzr}-\frac{a_{14}}{a_6}\tilde{H}_{zzr},\\
\tilde{\sigma}_{xyr} &= a_2q\tilde{u}_{xr}+a_2\sum_{k=1}^{N}X_{rk}^{(1)}\tilde{u}_{yk}+a_3q\tilde{w}_{xr}+a_3\sum_{k=1}^{N}X_{rk}^{(1)}\tilde{w}_{yk},\\
\tilde{H}_{xxr} &= a_1\sum_{k=1}^{N}X_{rk}^{(1)}\tilde{u}_{xk}+(a_{12}+a_3)q\tilde{u}_{yr}-a_{16}\sum_{k=1}^{N}X_{rk}^{(1)}\tilde{w}_{xk}+(a_{17}+a_4)q\tilde{w}_{yr}-\frac{a_{18}}{a_6}\tilde{\sigma}_{zzr}-\frac{a_{19}}{a_6}\tilde{H}_{zzr},\\
\tilde{H}_{yyr} &= a_1\sum_{k=1}^{N}X_{rk}^{(1)}\tilde{u}_{xk}+(a_{12}+a_3)q\tilde{u}_{yr}-a_{16}\sum_{k=1}^{N}X_{rk}^{(1)}\tilde{w}_{xk}+(a_{17}+a_4)q\tilde{w}_{yr}-\frac{a_{18}}{a_6}\tilde{\sigma}_{zzr}-\frac{a_{19}}{a_6}\tilde{H}_{zzr},\\
\tilde{H}_{xyr} &= a_3q\tilde{u}_{xr}+a_3\sum_{k=1}^{N}X_{rk}^{(1)}\tilde{u}_{yk}+a_4q\tilde{w}_{xr}+a_4\sum_{k=1}^{N}X_{rk}^{(1)}\tilde{w}_{yk}.
\end{aligned}
\tag{19}
$$

Three boundary conditions of SSSS, CSCS, CSSS, and CSFS are considered in this paper, and the state equations which satisfy the corresponding boundary conditions are listed in Eqs. (A.2)–(A.5) of "Appendix A".

The mechanical boundary conditions on the top and bottom surfaces of the plate can be expressed as

$$z = H : \tilde{\sigma}_{xzr} = \tilde{\sigma}_{yzr} = \tilde{H}_{xzr} = \tilde{H}_{yzr} = \tilde{H}_{zzr} = 0,\ \tilde{\sigma}_{zzr} = \sigma_0 \sin(\pi x_r / L_x) \sin qy,$$
$$z = 0 : \tilde{\sigma}_{xzr} = \tilde{\sigma}_{yzr} = \tilde{H}_{xzr} = \tilde{H}_{yzr} = \tilde{H}_{zzr} = 0,\ \tilde{\sigma}_{zzr} = k_w \tilde{u}_{zr} - k_g \left(\sum_{k=2}^{N-1} X_{rk}^{(2)} \tilde{u}_{zk} - q^2 \tilde{u}_{zr} \right), \tag{20}$$

where k_w and k_g are the Winkler layer and shearing layer elastic coefficients of the elastic medium; σ_0 is the phonon stress amplitude.

For the pth layer of the plate, Eq. (18) can be written in the following unified matrix form:

$$\frac{\mathrm{d}}{\mathrm{d}z} \boldsymbol{\delta}^{(p)} = \mathbf{T}^{(p)} \boldsymbol{\delta}^{(p)}, \tag{21}$$

where $\boldsymbol{\delta}^{(p)} = [\mathbf{u}_x^{\mathrm{T}}, \mathbf{u}_y^{\mathrm{T}}, \mathbf{w}_x^{\mathrm{T}}, \mathbf{w}_y^{\mathrm{T}}, \boldsymbol{\sigma}_{zz}^{\mathrm{T}}, \mathbf{H}_{zz}^{\mathrm{T}}, \boldsymbol{\sigma}_{xz}^{\mathrm{T}}, \boldsymbol{\sigma}_{yz}^{\mathrm{T}}, \mathbf{H}_{xz}^{\mathrm{T}}, \mathbf{H}_{yz}^{\mathrm{T}}, \mathbf{u}_z^{\mathrm{T}}, \mathbf{w}_z^{\mathrm{T}}],$, such as $\mathbf{u}_x^{\mathrm{T}} = \tilde{u}_{xr}$; $\mathbf{T}^{(p)}$ is the coefficient matrix of the pth layer at the appropriate discrete points.

According to the theory of ordinary differential equations, the general solution of Eq. (21) is

$$\boldsymbol{\delta}^{(p)}(z) = \exp\left[\mathbf{T}^{(p)}(z - z_{p-1})\right] \boldsymbol{\delta}^{(p)}(z_{p-1}) \quad (z_{p-1} \le z \le z_p). \tag{22}$$

Letting $z = z_p$ in Eq. (22), we find that

$$\boldsymbol{\delta}_1^{(p)+} = \mathbf{M}^{(p)} \boldsymbol{\delta}_0^{(p)-}, \tag{23}$$

where $\mathbf{M}^{(p)} = \exp\left[(z_p - z_{p-1})\mathbf{T}^{(p)}\right] = \exp\left[h_p \mathbf{T}^{(p)}\right]$, and '$-$' and '$+$' represent the lower and upper surface of the pth layer, respectively.

If the interfaces are in perfect bonding condition, the z-direction tractions and displacements are continuous through this interface, the propagator relation can be expressed as

$$\boldsymbol{\delta}_1^{(M)+} = \mathbf{P}_0^{(1)-}, \tag{24}$$

where the matrix $\mathbf{P} = \mathbf{M}^{(M)} \mathbf{M}^{(M-1)} \cdots \mathbf{M}^{(p)} \cdots \mathbf{M}^{(1)} = \prod_{p=M}^{1} \mathbf{M}^{(p)}$ is the total propagator matrix.

Equation (24) can be rewritten as

$$\boldsymbol{\delta}_1^{(M)} = \begin{bmatrix} \mathbf{U}(H) \\ \mathbf{Y}(H) \end{bmatrix} = \begin{bmatrix} \mathbf{P}_{11} & \mathbf{P}_{12} \\ \mathbf{P}_{21} & \mathbf{P}_{22} \end{bmatrix} \boldsymbol{\delta}_0^{(1)} = \begin{bmatrix} \mathbf{P}_{11} & \mathbf{P}_{12} \\ \mathbf{P}_{21} & \mathbf{P}_{22} \end{bmatrix} \begin{bmatrix} \mathbf{U}(0) \\ \mathbf{Y}(0) \end{bmatrix}, \tag{25}$$

where $\mathbf{U}(z) = \left[\mathbf{u}_x^{\mathrm{T}}, \mathbf{u}_y^{\mathrm{T}}, \mathbf{u}_z^{\mathrm{T}}, \mathbf{w}_x^{\mathrm{T}}, \mathbf{w}_y^{\mathrm{T}}, \mathbf{w}_z^{\mathrm{T}}\right]^{\mathrm{T}}$, $\mathbf{Y}(z) = \left[\boldsymbol{\sigma}_{xz}^{\mathrm{T}}, \boldsymbol{\sigma}_{yz}^{\mathrm{T}}, \boldsymbol{\sigma}_{zz}^{\mathrm{T}}, \mathbf{H}_{xz}^{\mathrm{T}}, \mathbf{H}_{yz}^{\mathrm{T}}, \mathbf{H}_{zz}^{\mathrm{T}}\right]^{\mathrm{T}}$.

Incorporating Eq. (20) with Eq. (25), the solution of the FG 3D cubic QC laminate can be obtained.

3 Numerical examples

In this Section, some typical numerical examples are presented for the static response of the FG multilayered 3D cubic QC plates on an elastic foundation with mixed boundary conditions. The multilayer plate is composed of three single plates, and each layer has the same thickness. The dimensions of the plates are $L_x \times L_y \times H = 1\ \mathrm{mm} \times 1\ \mathrm{mm} \times 0.3\ \mathrm{mm}$. According to the QC material coefficients shown in literature [29], two kinds of material properties (QC1 and QC2) are listed in Table 1. These material parameters completely match the QC elastic deformation energy density [30, 34], so they can be used to simulate the variation of the QC plates. For the FGM laminate, five different exponential factors ($\eta = -10, -5, 0, 5, 10$) are investigated, and the material properties of each layer are exponential distributions along the thickness direction shown in Fig. 2. In this paper, the elastic coefficients are defined as $k_w = K_w \times C_{\max}/L_x$ and $k_g = K_g \times C_{\max} \times H$, where $C_{\max}$ is the maximum elastic coefficient of the bottom surface of the plate.

Table 1 Material properties (C^0_{mn}, K^0_{mn}, and R^0_i in 10^9 N/m^2)

	C^0_{11}	C^0_{12}	C^0_{44}	K^0_{11}	K^0_{12}	K^0_{44}	R^0_1	R^0_2	R^0_3
QC1	112.1	60.3	32.8	60	20	10	5	− 2	7
QC2	40	20	30	10	7	6	− 1	0.7	3

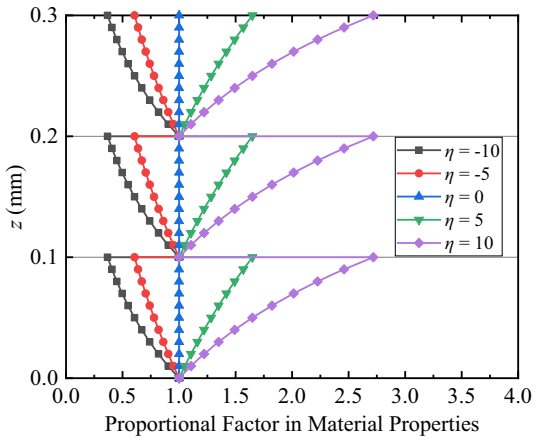

Fig. 2 Variation of the FGM proportional coefficients for $\eta = -10, -5, 0, 5$, and 10

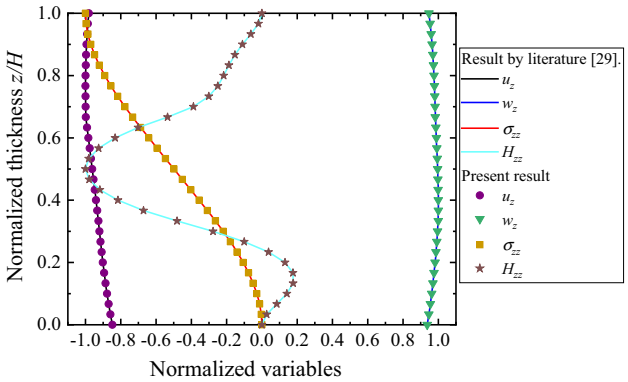

Fig. 3 Normalized displacements and stresses for the QC1/QC2/QC1 plate

3.1 Validation

In order to verify the validity and accuracy of SS-DQM, a 3D cubic QC laminate with simply supported boundary conditions is considered. The material elastic coefficients, the shape and size, and loading and boundary conditions for this plate are consistent with those in the literature [29]. In addition, the FG exponential factor is taken as $\eta = 0$, the foundation parameters are taken as $K_w = K_g = 0$, and the horizontal coordinate is fixed at $(x, y) = (0.75L_x, 0.75L_y)$. The phonon displacement u_z, phason displacement w_z, phonon stress σ_{zz}, and phason stress H_{zz} are normalized by their maximum among these four variables along the thickness direction. Figure 3 shows the variation of the displacements and stresses for the QC1/QC2/QC1 plate with continuous interface conditions under the mechanical load. It can be proved that the solutions by using SS-DQM are in good agreement with the results of the literature [29]. Thus, the method in this paper has high precision and good convergence.

In the above calculation process, the discrete points are taken as $N = 13$. However, for the different discrete points N, the values of the relative error t of the field variables are listed in Table 2.

The relative error t is defined as

$$t = \frac{\alpha_1 - \alpha_2}{\alpha_1} \times 100\%, \tag{26}$$

Table 2 The relative error t (%)

H	N	u_x	u_z	w_x	w_z	σ_{xz}	H_{xz}	σ_{xx}	H_{xx}
0.1	5	1.406915	0.498020	1.137555	0.384173	1.307458	2.964223	0.091961	0.050030
	7	0.017277	0.000979	0.015903	0.001006	0.016753	0.070485	0.000492	0.000233
	9	0.000140	0.000011	0.000132	0.000011	0.000137	0.000161	0.000004	0.000002
	11	0	0	0.000001	0	0.000001	0.000001	0	0
0.3	5	1.492743	0.540788	1.166653	0.486494	1.311766	4.620004	0.177884	0.061949
	7	0.017762	0.001016	0.018108	0.001031	0.016940	0.126172	0.001704	0.000292
	9	0.000148	0.000014	0.000141	0.000019	0.000146	0.000184	0.000011	0.000004
	11	0.000001	0	0.000001	0	0.000001	0.000002	0	0
0.5	5	1.554029	0.600334	1.432899	0.331570	1.323954	6.398266	0.367182	0.075618
	7	0.017303	0.001087	0.022998	0.001045	0.017231	0.206222	0.002809	0.001638
	9	0.000157	0.000019	0.000150	0.000029	0.000155	0.000251	0.000013	0.000007
	11	0.000001	0.000001	0.000001	0.000001	0.000001	0.000003	0.000001	0.000001

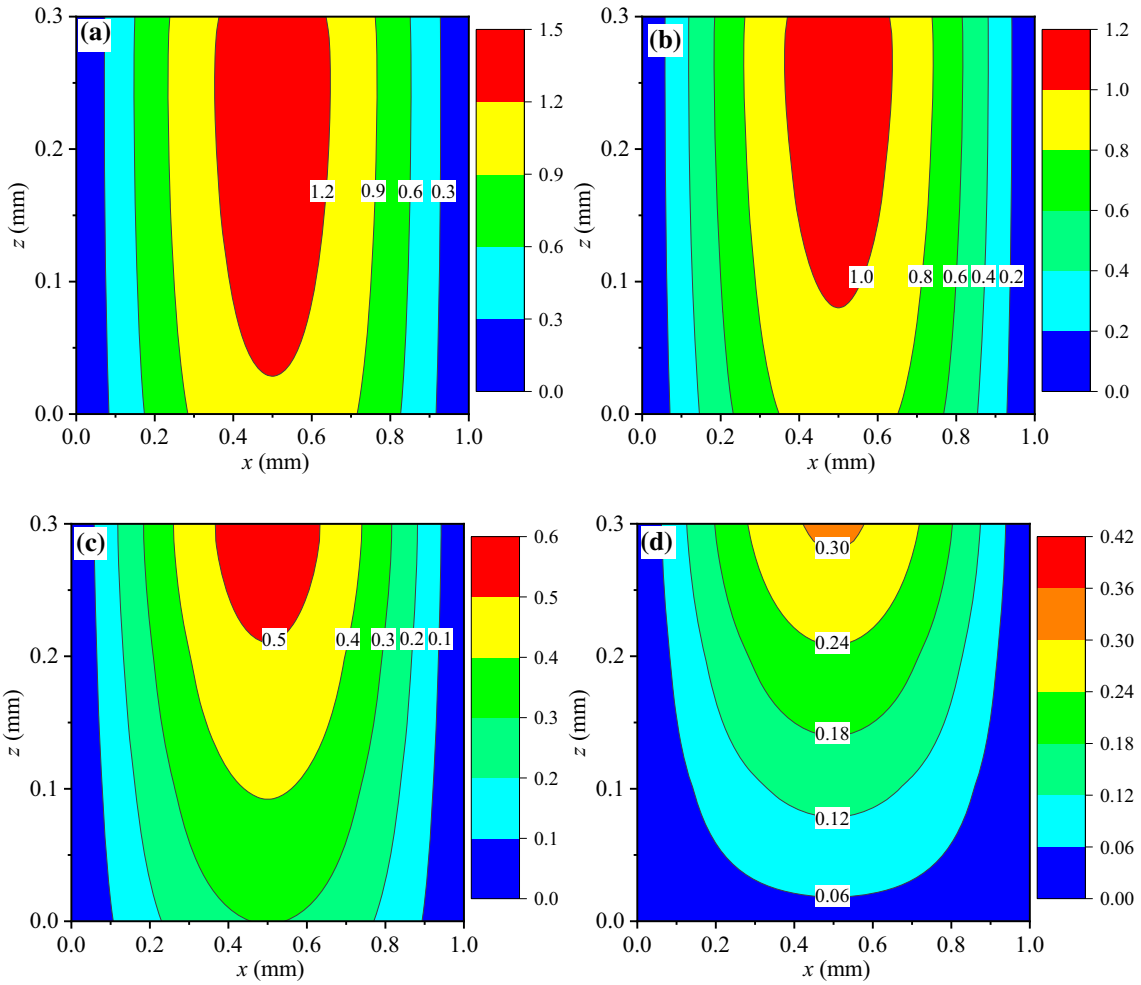

Fig. 4 Effect of the K_g on the phonon displacement u_z (10^{-12} mm): **a** $K_g = 0$, **b** $K_g = 0.01$, **c** $K_g = 0.1$, and **d** $K_g = 1$

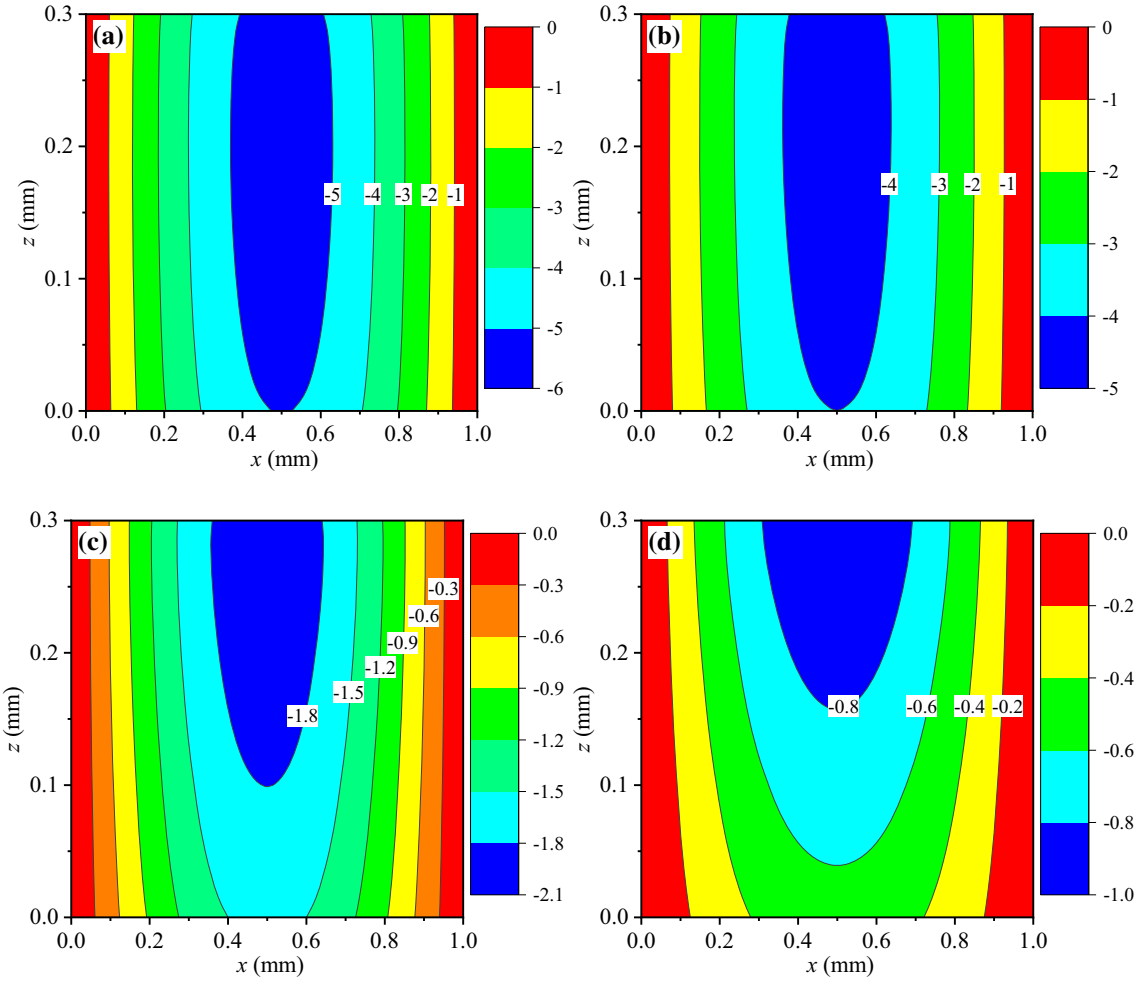

Fig. 5 Effect of the K_g on the phason displacement w_z (10^{-12} mm): **a** $K_g = 0$, **b** $K_g = 0.01$, **c** $K_g = 0.1$, and **d** $K_g = 1$

where α_1 is the exact solution of the plate in the literature [29]; α_2 is the solution of SS-DQM for the plate when N is given.

As shown in Table 2, '0' denotes $t \leq 0.0000005\%$. The maximal relative error of the present solution at $N = 11$ is only about $t = 0.000003\%$ for the solution in the literature [29]. Thus, this high-precision method can be used to satisfy the requirements. Furthermore, for the same thickness of the plates, the solutions become more accurate with the increase of N. However, when $N \geq 23$, numerical instability is encountered. In addition, with the increase of the plate thickness, the values of t keep getting larger. This feature indicates that the high aspect ratio of H/L_y will cause numerical instability. Thus, numerical instabilities are always encountered during the present solution procedure in the case of the high aspect ratio of H/L_y and large discrete point number N. In order to ensure the accuracy and convergence of this method, the discrete points are taken as $N = 13$ in the following examples.

3.2 The effect of the elastic coefficients on FG QC plates with boundary condition SSSS

In this part, we present the solution of the FG QC1/QC1/QC1 plate on an elastic foundation with boundary conditions SSSS. The FG exponential factor is set as $\eta = 5$. The foundation parameters are taken as $K_w = 0.1$ and $K_g = 0, 0.01, 0.1$, and 1.

Figures 4 and 5 present the contour plots of u_z and w_z for the plate on the x–z plane with $y = 0.5L_y$, respectively. The maximum magnitudes of u_z (Fig. 4a–d) and w_z (Fig. 5a–d) exist at the center of the x–y plane and decrease with the increase of K_g. This feature indicates that K_g has a large effect on u_z, and w_z, and the

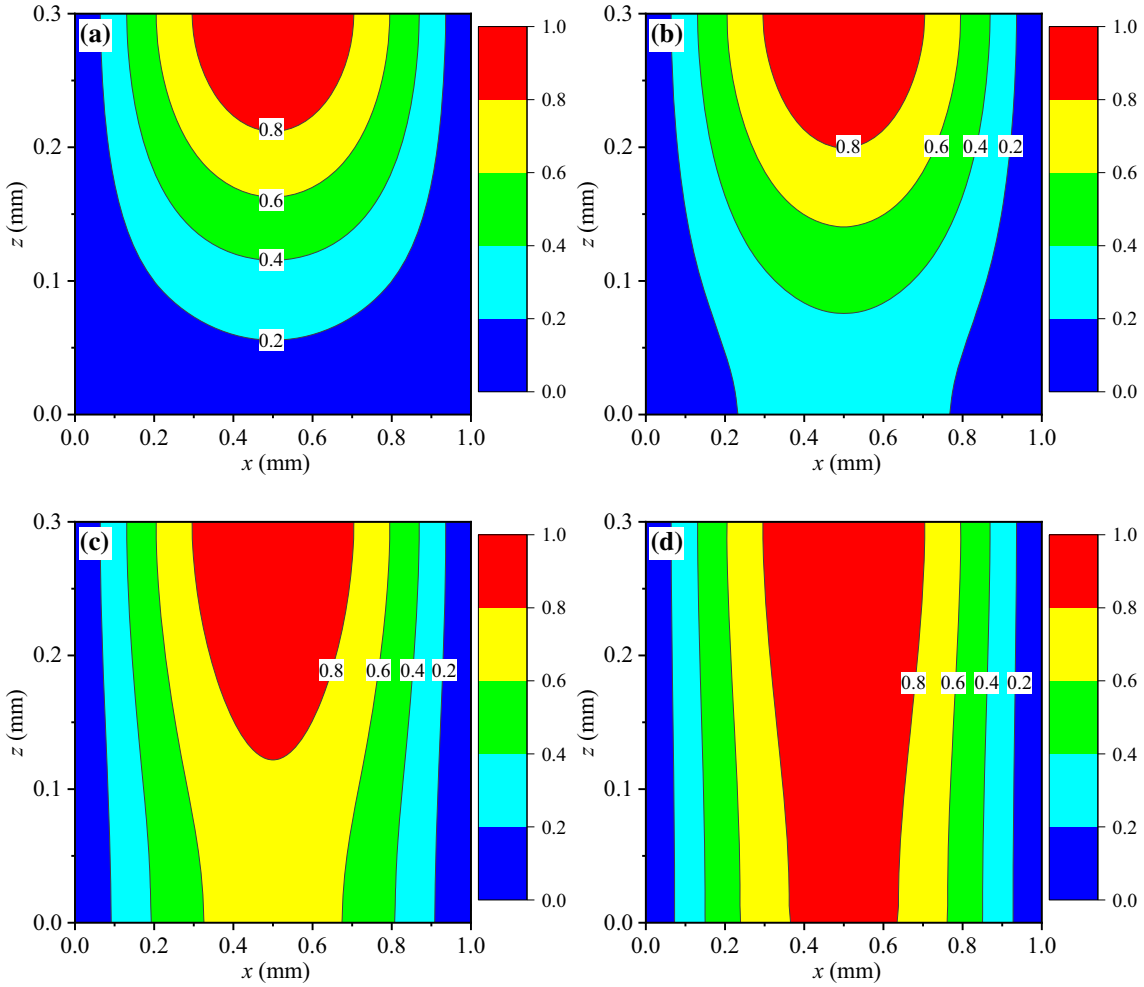

Fig. 6 Effect of the K_g on the phonon stress σ_{zz} (N/m^2): **a** $K_g = 0$, **b** $K_g = 0.01$, **c** $K_g = 0.1$, and **d** $K_g = 1$

rigidity of the plate is constantly getting stronger. The distributions of u_z and w_z of the plate are symmetric at $x = 0.5$ mm. It is observed that the magnitude of w_z is larger than that of u_z with the increase of K_g, so K_g has a larger impact on w_z.

Figures 6 and 7 present the contour plots of σ_{zz} and H_{zz} for the plate on the x–z plane with $y = 0.5L_y$, respectively. σ_{zz} (Figs. 6 (a)-(d)) and H_{zz} (Figs. 7 (a)-(d)) obviously change with the different K_g, and they are sensitive to the values of K_g. The negative values of H_{zz} occur at $0 < K_g < C_{\max}$. In addition, stress concentration appears in the distribution of H_{zz} (Fig. 7 (b)). Thus, H_{zz} is sensitive to the K_g, and the distribution of H_{zz} exhibits special characteristics. The values of K_g have a significant influence on σ_{zz} and H_{zz}.

3.3 The effect of FG exponential factors on FG QC plates with boundary condition CSCS

In this part, we present the solution of the FG QC1/QC2/QC1 plate on an elastic foundation with boundary conditions CSCS. The FG exponential factors are set as $\eta = -10, -5, 0, 5$, and 10. The foundation parameters are taken as $K_w = 0.2$ and $K_g = 0.02$. To show the distribution of field variables along the thickness direction, the horizontal coordinate is fixed at $(x, y) = (0.25L_x, 0.5L_y)$.

The variation of the phonon and phason displacements of the plate along the thickness direction under the mechanical load is presented in Fig. 8. On the top and bottom surfaces of the plate, the absolute values of these displacements (Figs. 8 (a)-(f)) decrease with the increase of η. Different from the plate with boundary condition SSSS, the values of u_x and u_y (Figs. 8 (a) and (b)) are not equal since the plate has different boundary conditions. The distribution of u_z (Fig. 8 (c)) decreases with the increase of η. This feature indicates that the

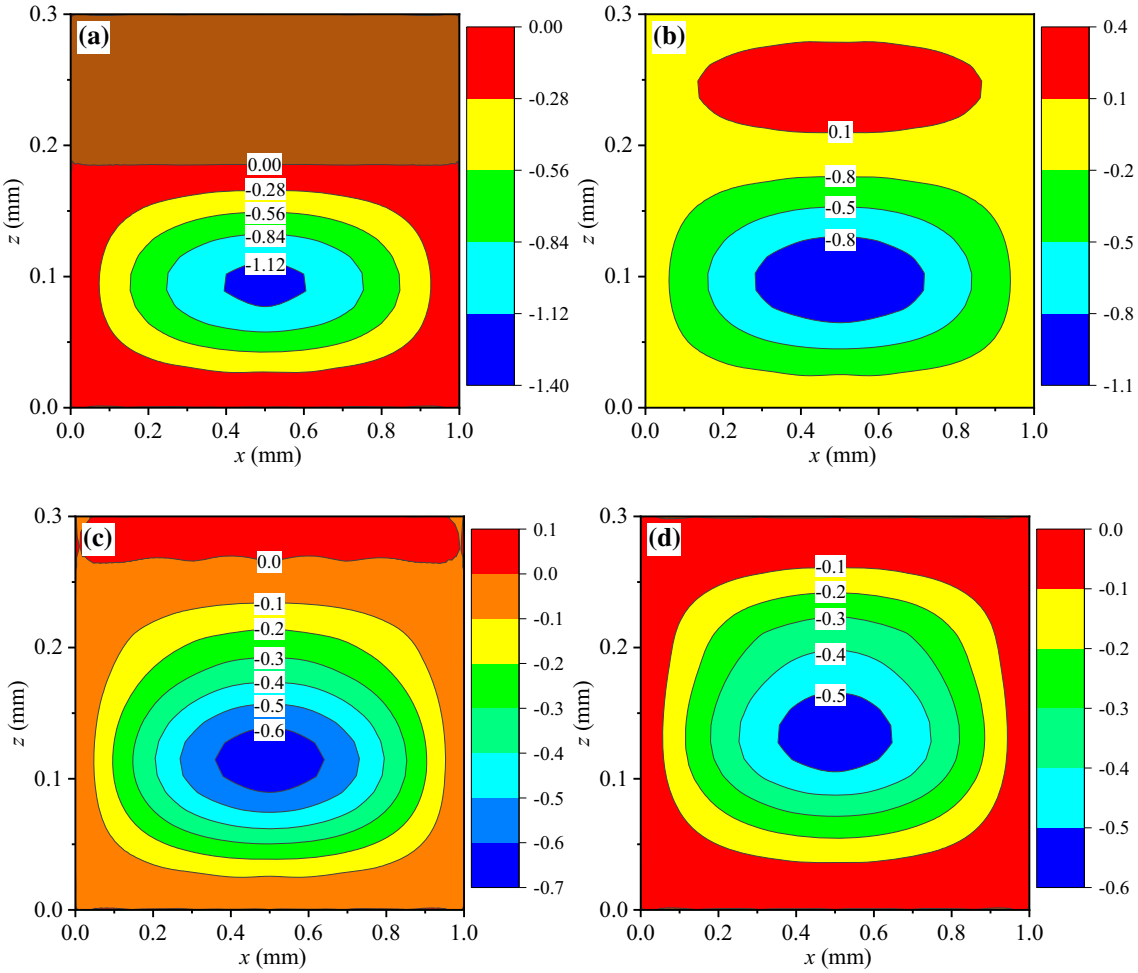

Fig. 7 Effect of the K_g on the phonon stress H_{zz} (10^{-3} N/m^2): **a** $K_g = 0$, **b** $K_g = 0.01$, **c** $K_g = 0.1$, and **d** $K_g = 1$

rigidity of the plate is constantly getting stronger. As same as u_x and u_y, the values of w_x (Fig. 8 (d)) and w_y (Fig. 8 (e)) are also not equal. Meanwhile, the value of w_y is less affected by η than that of w_x. The distribution of w_z (Fig. 8 (f)) has a large variation with the difference of η, and w_z is sensitive to η.

The variation of the phonon and phason stresses of the plate along the thickness direction under the mechanical load is presented in Fig. 9. σ_{xx} is discontinuous between different material layers in Fig. 9 (a). Based on the classic laminate theory, only the local stress of the basic equation of the QC is considered. But in fact, the stress state also includes the strong interlayer stress between the interfaces. The high-interlayer stress is considered to be one of the special failure mechanisms of composite materials in engineering applications. The values of σ_{xz} and σ_{yz} (Figs. 9 (b) and (c)) increase with the increase of η at $z = 0.15$ mm. H_{xx} (Fig. 9 (d)) is discontinuous at $z = 0.1$ mm, and the interlayer stress value decreases with the increase of η. The values of H_{xz} and H_{yz} (Figs. 9 (e) and (f)) increase with the increase of η at $z = 0.2$ mm.

3.4 The effect of the stacking sequence on FG QC plates with boundary condition CSSS

In this part, we present the solution of six kinds of stacking sequence plates (QC1/QC1/QC1, QC1/QC1/QC2, QC1/QC2/QC1, QC2/QC1/QC2, QC2/QC2/QC1, and QC2/QC2/QC2,) on an elastic foundation with boundary conditions CSSS. The FG exponential factor is set as $\eta = -5$. The foundation parameters are taken as $K_w = K_g = 0$. To show the distribution of the field variables along the thickness direction, the horizontal coordinate is fixed at $(x, y) = (L_x, 0.5L_y)$.

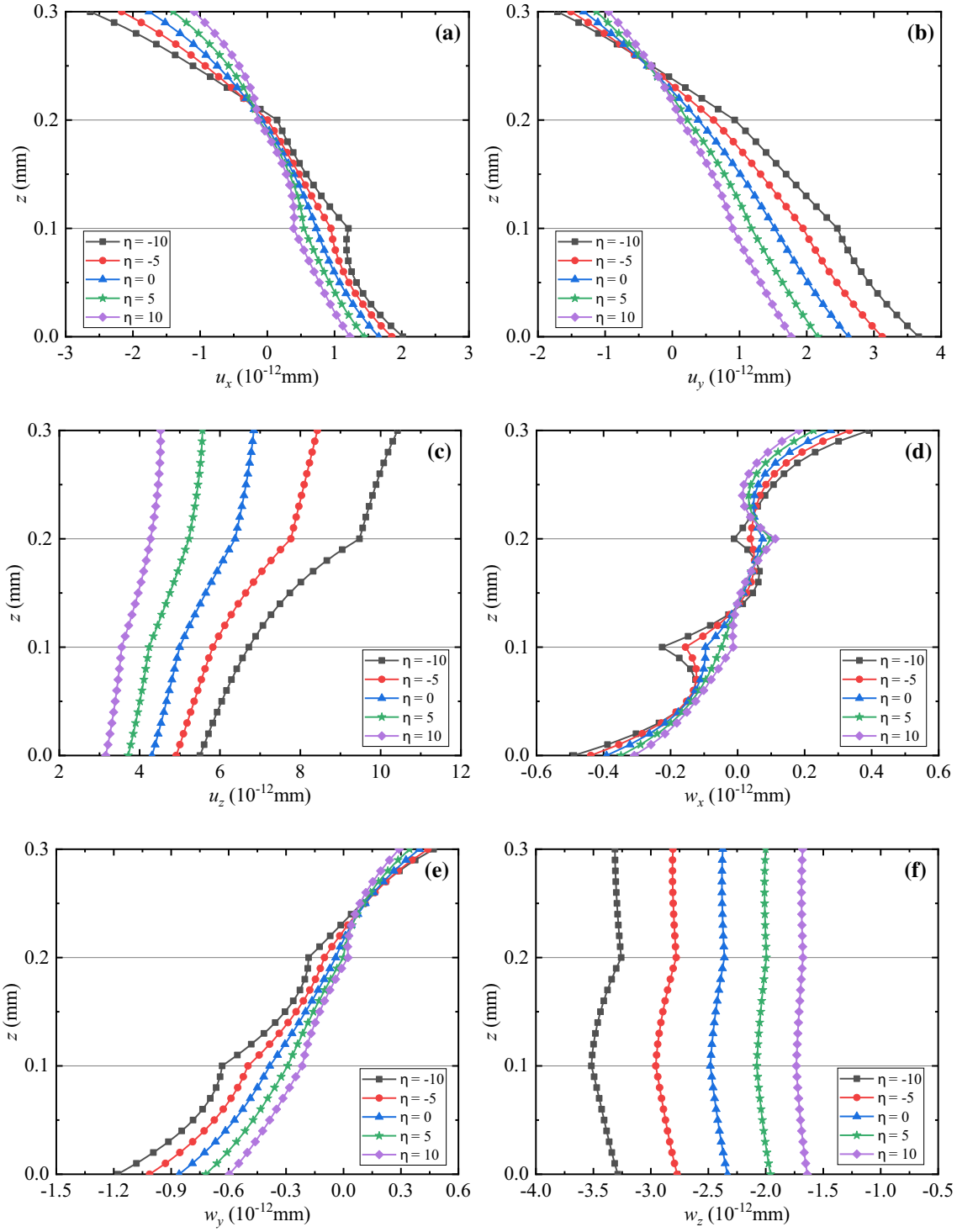

Fig. 8 Variation of the phonon and phason displacements for a QC1/QC2/QC1 plate: **a** u_x, **b** u_y, **c** u_z, **d** w_x, **e** w_y, and **f** w_z

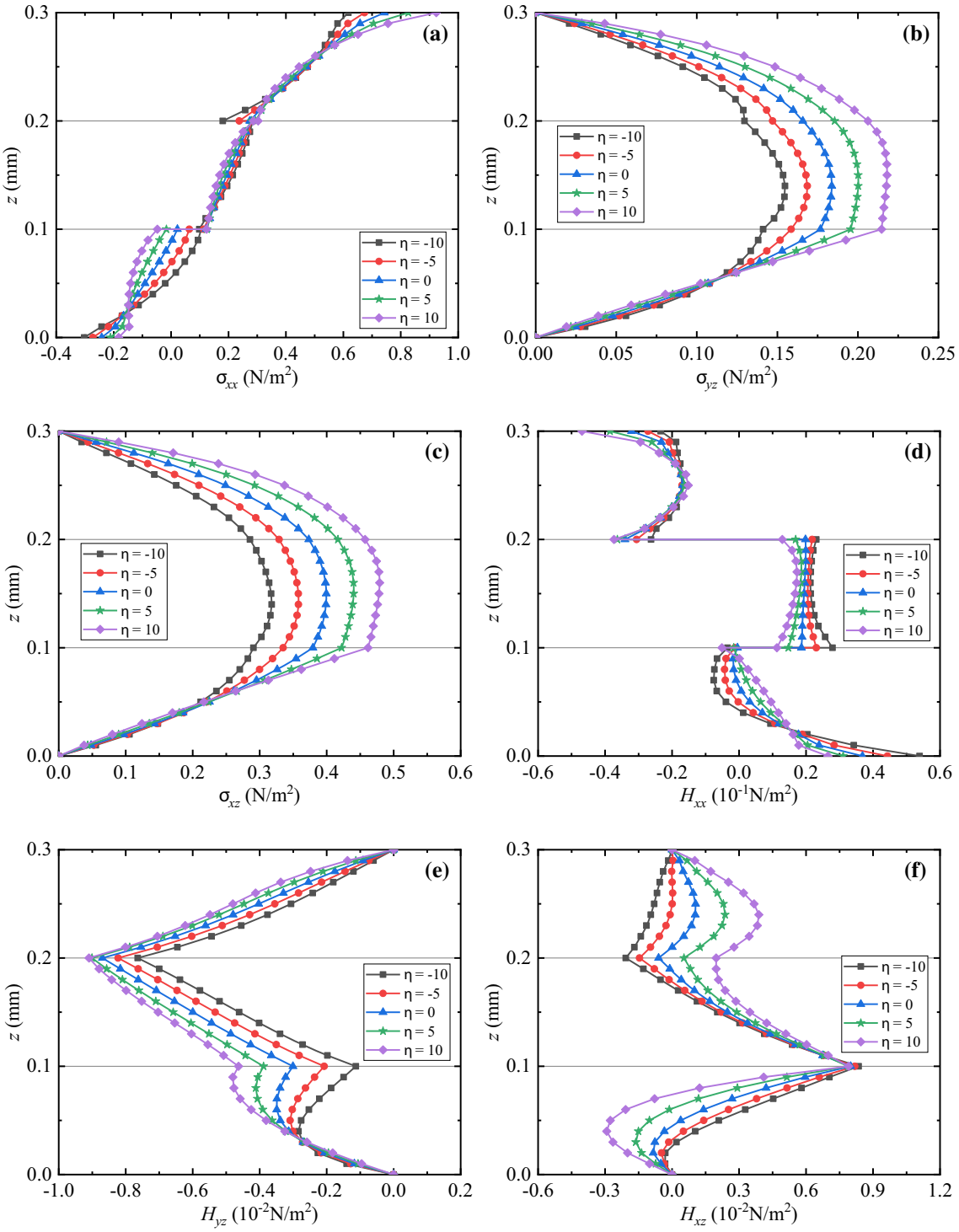

Fig. 9 Variation of the phonon and phason stresses for a QC1/QC2/QC1 plate: **a** σ_{xx}, **b** σ_{yz}, **c** σ_{xz}, **d** H_{xx}, **e** H_{yz}, and **f** H_{xz}

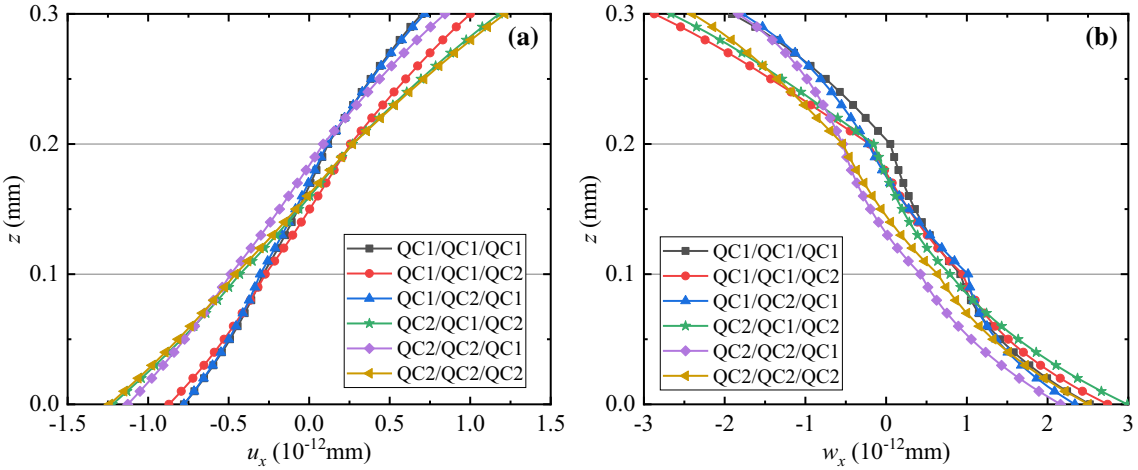

Fig. 10 Variation of the phonon and phason displacements for six kinds of plates: **a** u_x and **b** w_x

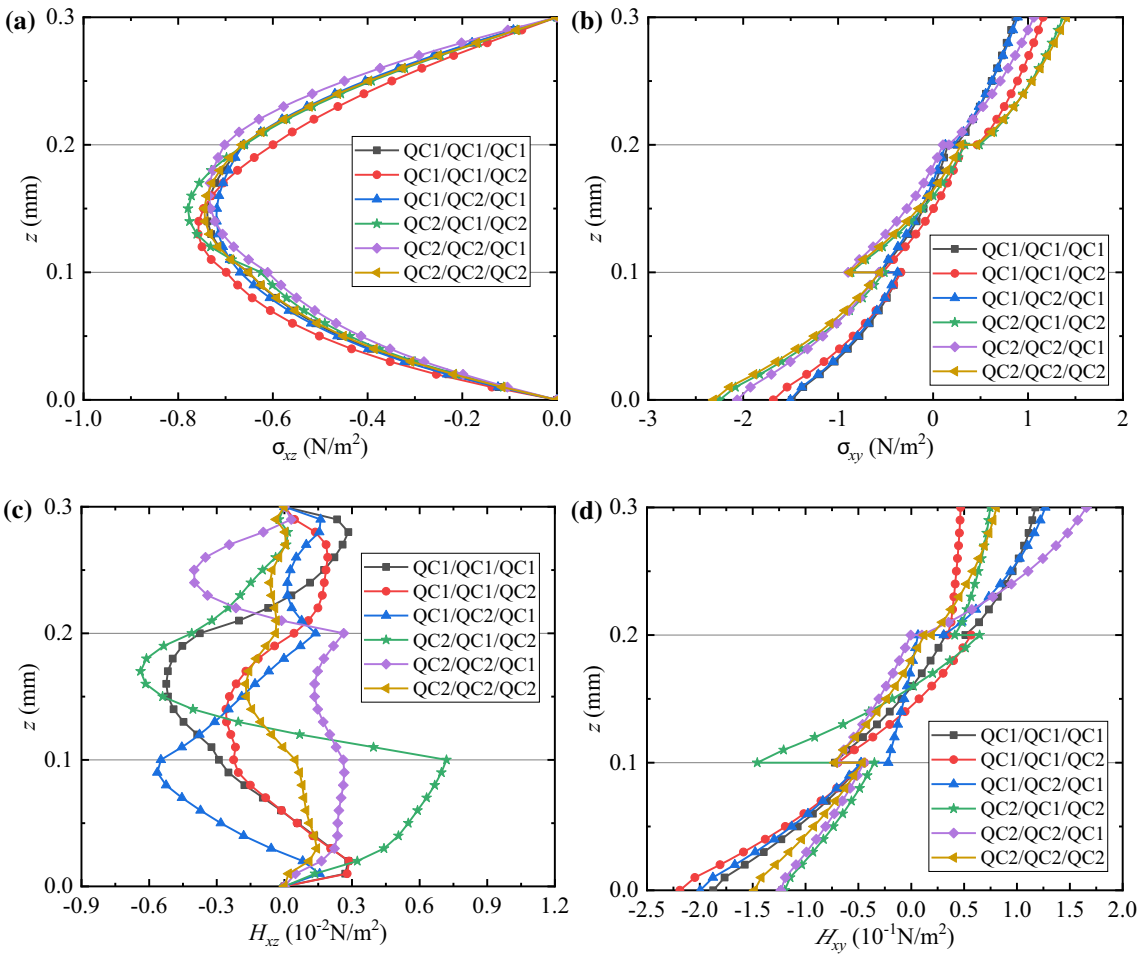

Fig. 11 Variation of the phonon and phason stresses for six kinds of plates: **a** σ_{xz}, **b** σ_{xy}, **c** H_{xz}, and **d** H_{xy}

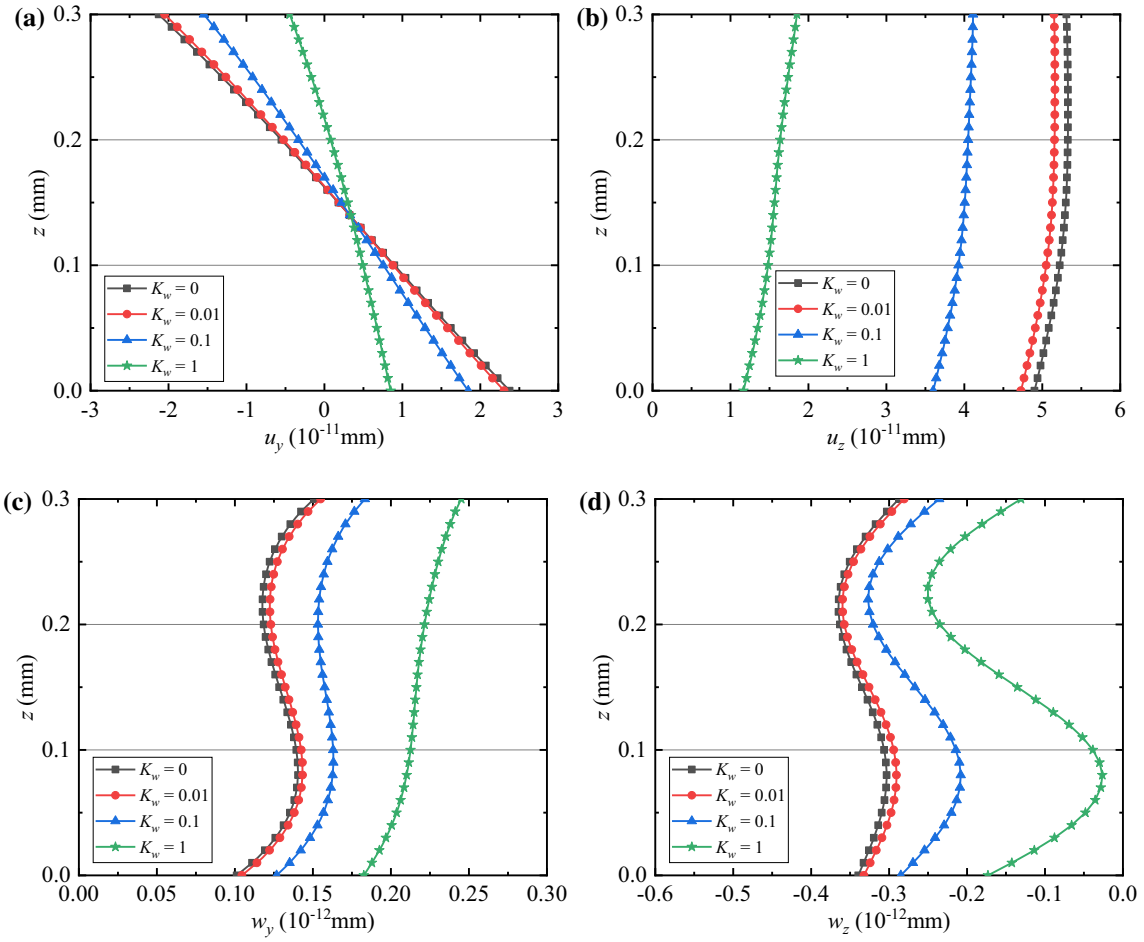

Fig. 12 Variation of the phonon and phason displacements for a QC2/QC2/QC2 plate: **a** u_y, **b** u_z, **c** w_y, and **d** w_z

The variation of the phonon and phason displacements of these plates along the thickness direction under the mechanical load is presented in Fig. 10. It can be observed that u_x and w_x (Figs. 10 (a) and (b)) are continuous at the interface between layers. Furthermore, the stacking sequence has little effect on u_x and w_x and does not change their magnitude and direction at the top and bottom surfaces of the laminates. It should be noted that the responses of u_y, u_z, w_y, and w_z are not given because their values are zero at $x = L_x$. This feature is consistent with the linear elastic theory of QCs.

The variation of the phonon and phason stresses of these plates along the thickness direction under the mechanical load is presented in Fig. 11. The solution strictly satisfies the basic equation of 3D cubic QC, and the distribution of field variables at any position of the plate can be presented. Here, Figs. 11 (a)-(d) present the accurate stress solutions at $x = L_x$, which also indicates that these solutions have theoretical significance. The distribution of σ_{xz} along the z-direction is not symmetrical in Fig. 11 (a). The distributions of these stresses at $x = L_x$ are consistent with the in-plane distribution trend, and the value is larger at the boundary. σ_{xy} (Fig. 11 (b)) is the same as σ_{xx} and σ_{yy}, which is discontinuous between different material layers. If the material properties of each layer are the same, the stress is continuous for these plates. The stacking sequences have a larger impact on H_{xz} (Fig. 11 (c)), which changes the overall distribution of H_{xz}. Similarly, H_{yx} (Fig. 11 (d)) is discontinuous between two adjacent QC material layers. For the above physical variables, if DQM will be also utilized to discretize domains along the y-direction, the superposition l will not appear in the formulations of the exact solution.

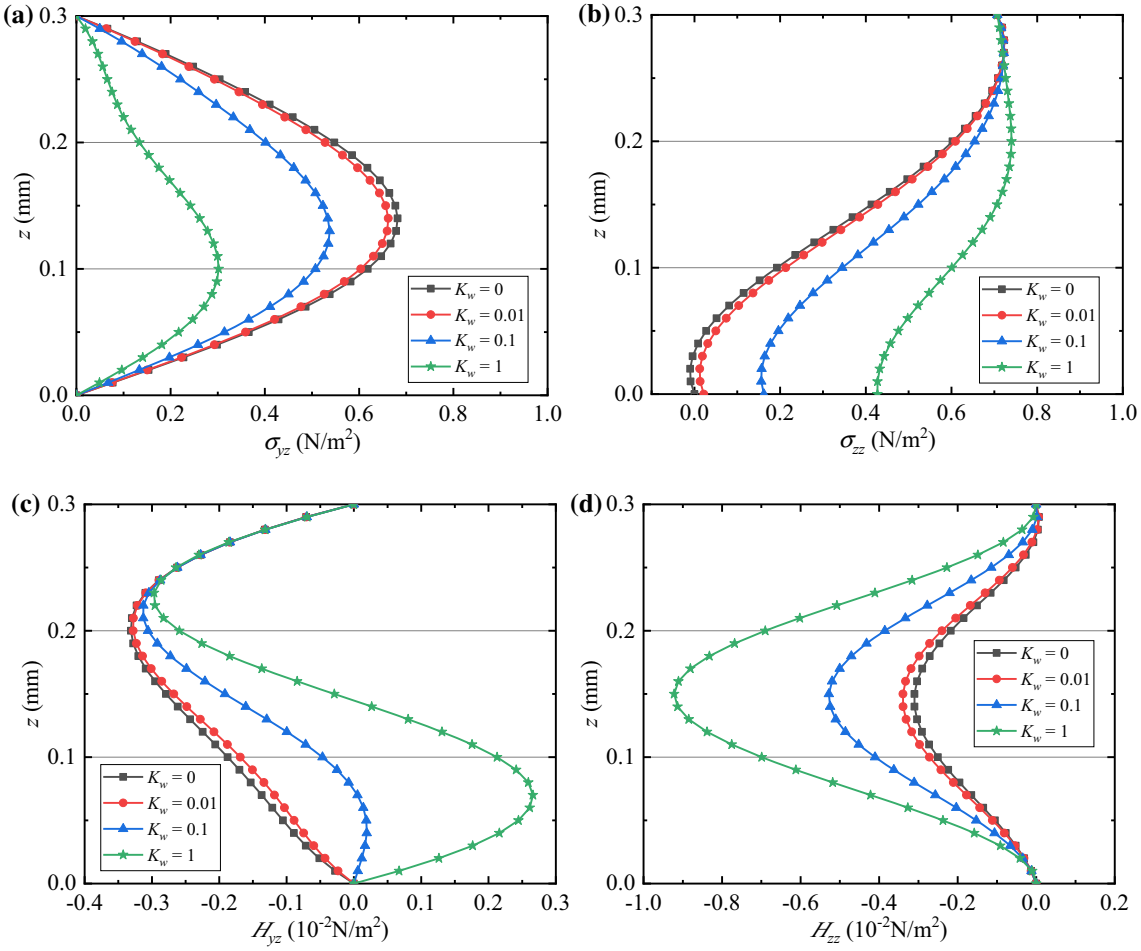

Fig. 13 Variation of the phonon and phason stresses for a QC2/QC2/QC2 plate: **a** σ_{yz}, **b** σ_{zz}, **c** H_{yz}, and **d** H_{zz}

3.5 The effect of the Winkler layer coefficients on FG QC plates with boundary condition CSFS

In this part, we present the solution of the QC2/QC2/QC2 plate on an elastic foundation with boundary conditions CSFS. The FG exponential factor is set as $\eta = 0$. The foundation parameters are taken as $K_w =$ 0, 0.01, 0.1, 1, and $K_g = 0$. To show the distribution of the field variables along the thickness direction, the horizontal coordinate is fixed at $(x, y) = (0.25L_x, 0.5L_y)$.

The variation of the phonon and phason displacements of the plate along the thickness direction under the mechanical load is presented in Fig. 12. With the increase of K_w, the value of u_y and u_z (Figs. 12 (a) and (b)) on the bottom and top surface keep decreasing, but the value of w_y and w_z (Figs. 12 (c) and (d)) increases. The displacements are sensitive to K_w, and the overall distributions of displacements along the thickness direction are changed at $K_w = 1$.

The variation of the phonon and phason stresses of the plate along the thickness direction under the mechanical load is presented in Fig. 13. With the increase of K_w, the stiffness of the foundation gradually increases, and the amplitude of shear stress σ_{yz} (Fig. 13 (a)) gradually decreases. The maximum value of σ_{zz} (Fig. 13 (b)) is not on the top surface of this plate, and K_w changes the position of the maximum value in the plate. This feature indicates that the overall bending stiffness of the laminate is continuously increasing due to the gradual stronger foundation stiffness. When $K_w = C_{\max}$, the overall distribution of H_{yz} (Fig. 13 (c)) is changed. The value of H_{zz} (Fig. 13 (d)) at $z = 0.15$ mm is the maximum, and K_w does not change the position of the maximum value in this plate.

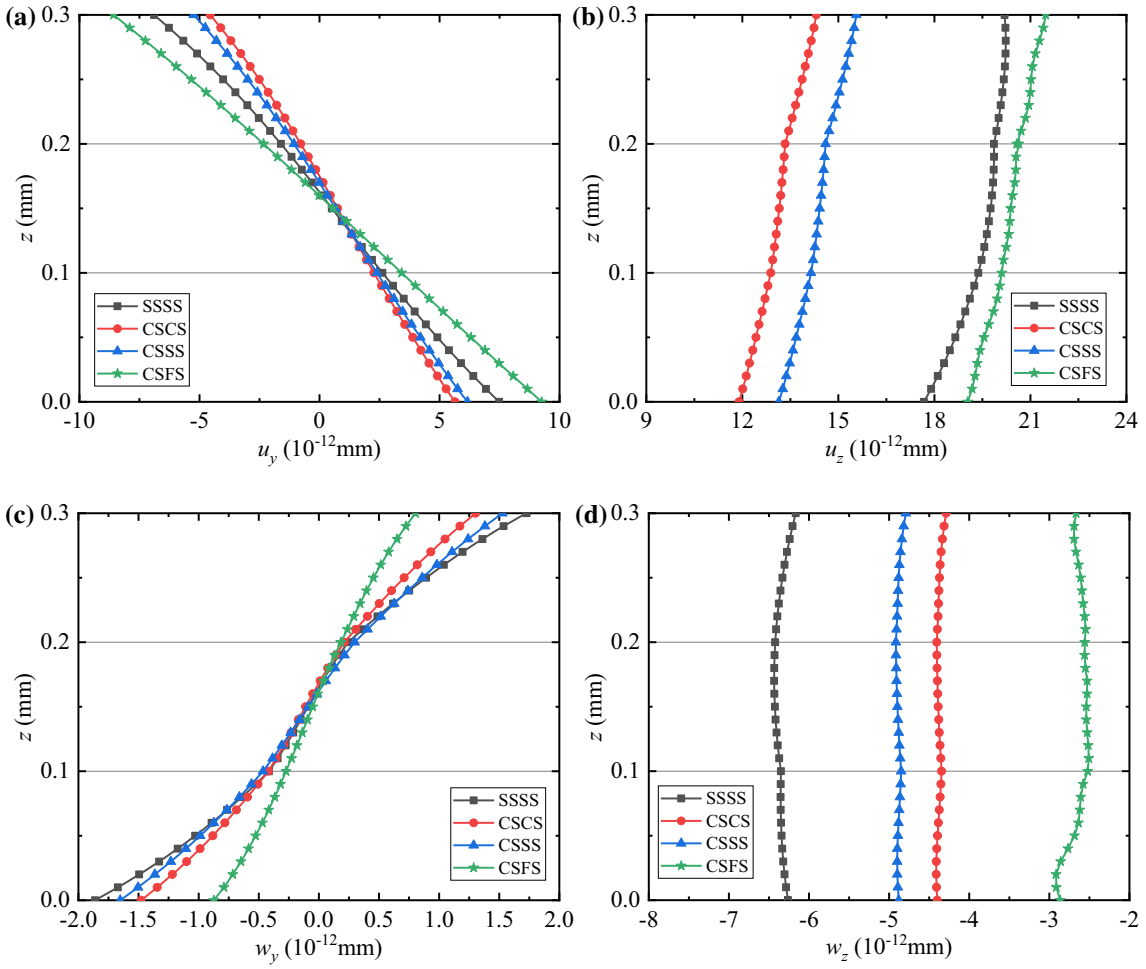

Fig. 14 Variation of the phonon and phason displacements for a QC2/QC1/QC2 plate: **a** u_y, **b** u_z, **c** w_y, and **d** w_z

3.6 FG QC laminate with boundary conditions SSSS, CSCS, CSSS, and CSFS

In this part, we present the solution of the FG QC2/QC1/QC2 plate on an elastic foundation with boundary conditions SSSS, CSCS, CSSS, and CSFS. The FG exponential factor is set as $\eta = 0$. The foundation parameters are taken as $K_w = K_g = 0$. To show the distribution of the field variables along the thickness direction, the horizontal coordinate is fixed at $(x, y) = (0.25L_x, 0.5L_y)$.

The variation of the phonon and phason displacements of the plate along the thickness direction under the mechanical load is presented in Fig. 14. It can be observed that the different boundary conditions have an obvious influence on u_y and w_y (Figs. 14 (a) and (c)). The maximum magnitudes of u_z (Fig. 14 (b)) exist at the top surface of the plate. In addition, u_z and w_z (Fig. 14 (d)) decrease with the increase of clamped-supported boundary conditions except for boundary condition CSFS. This feature indicates that the clamped-supported boundary conditions have a larger effect on u_z and w_z, and the rigidity of the plate is constantly getting stronger.

The variation of the phonon and phason stresses of the plate along the thickness direction under the mechanical load is presented in Fig. 15. The value of σ_{yz} (Fig. 15 (a)) with boundary conditions SSSS is larger than that of σ_{yz} with CSCS, CSSS, and CSFS. This feature indicates that the clamped-supported boundary conditions are more constrained than the simply supported edge for the phonon stresses, and it can bear more load. The maximum value of σ_{zz} (Fig. 15 (b)) is not on the top surface of this plate, and σ_{zz} is sensitive to the free-supported boundary condition. The distribution of H_{zz} (Fig. 15 (d)) with SSSS is significantly different from that of H_{zz} with CSCS, CSSSS, and CSFS.

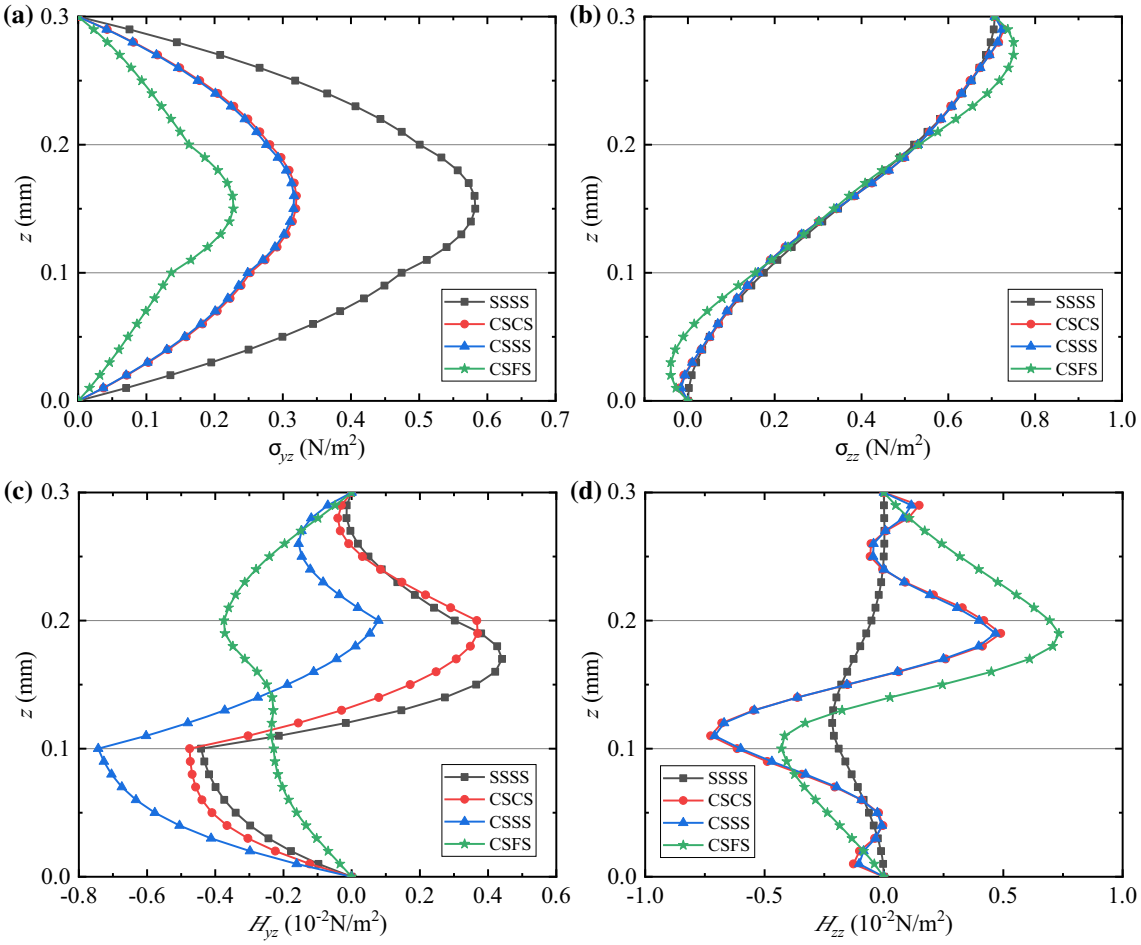

Fig. 15 Variation of the phonon and phason stresses for a QC2/QC1/QC2 plate: **a** σ_{yz}, **b** σ_{zz}, **e** H_{yz}, and **f** H_{zz}

4 Conclusions

In this paper, the related formulations of the static response of FG multilayered 3D cubic QC thick plates on an elastic foundation based on the linear elastic theory of QCs were derived using the SS-DQM. Since no assumptions on stresses and displacements have been employed, DQM has the superiority to yield results for FG plates with clamped-supported or simply supported boundary conditions. Using the state-space method along the thickness direction further allows one to deal with FG plates with an arbitrary thickness distribution of the material properties. The propagator matrix can be applied to connect the field variables at the upper and lower interfaces of each layer. Making use of the top surface boundary condition and the elastic foundations as a boundary condition on the bottom surface, the static solutions can be derived from the global propagator matrix. The numerical examples are presented to verify the accuracy of SS-DQM and illustrate the influence of different boundary conditions, stacking sequence, foundation parameters, and FG exponential factor on the phonon and phason variables. Finally, some significant features are listed below:

(i) Numerical examples in the literature prove that SS-DQM has high precision and good convergence in this paper. In addition, it is proved that the high aspect ratio of H/L_y and large discrete point number N are the causes of numerical instability.

(ii) The elastic coefficients K_w, K_g, and FG exponential factor η have a larger effect on the displacements u_z and w_z, and the rigidity of the plate is constantly getting stronger with the increase of K_w, K_g, and η.

(iii) The stresses σ_{xx}, σ_{yy}, σ_{xy}, H_{xx}, H_{yy}, and H_{yz} are discontinuous at the interface between the layers when the materials of two adjacent layers of the laminated board are different. This interface stress discontinuity is affected by the strong interlayer stress. Furthermore, K_g, K_w, and η have a larger effect on these stresses.

The semi-analytical method constructed in this paper is of high precision and fast convergence for deriving the solutions of the FG 3D cubic QC laminates with mixed boundary conditions. Some special cases such as multi-field coupled QC, FG 1D, 2D QC, and piezoelectric QC plates could all be investigated according to the present solutions. Furthermore, the methods and numerical results in this paper can be utilized to validate the accuracy of other numerical methods and serve for the analysis and design of intelligent QC material laminates.

Funding This work was supported by the National Natural Science Foundation of China (Grant Numbers 11972365, 12102458, and 11972354) and China Agricultural University Education Foundation (Grant Number 1101-240001).

Appendix A

Some parameters

$$
\begin{aligned}
&a_1 = C_{44}^0 K_{44}^0 - R_3^0 R_3^0, \quad a_2 = C_{44}^0, \quad a_3 = R_3^0, \quad a_4 = K_{44}^0, \quad a_5 = \frac{C_{11}^0}{C_{11}^0 K_{11}^0 - R_1^0 R_1^0}, \quad a_6 = C_{11}^0 K_{11}^0 - R_1^0 R_1^0,\\
&a_7 = C_{11}^0 R_2^0 R_2^0 + C_{12}^0 C_{12}^0 K_{11}^0 - 2C_{12}^0 R_1^0 R_2^0, \quad a_8 = -C_{11}^0 + \frac{a_7}{a_6}, \quad a_9 = -C_{12}^0 - C_{44}^0 + \frac{a_7}{a_6},\\
&a_{10} = C_{11}^0 K_{12}^0 R_2^0 - C_{12}^0 R_1^0 K_{12}^0 + C_{12}^0 R_2^0 K_{11}^0 - R_1^0 R_2^0 R_2^0, \quad a_{11} = \frac{a_{10}}{a_6} - R_1^0, a_{12} = \frac{a_{10}}{a_6} - R_2^0 - R_3^0,\\
&a_{13} = -C_{12}^0 K_{11}^0 + R_1^0 R_2^0, a_{14} = -C_{11}^0 R_2^0 + C_{12}^0 R_1^0, \quad a_{15} = C_{11}^0 K_{12}^0 K_{12}^0 - 2K_{12}^0 R_1^0 R_2^0 + K_{11}^0 R_2^0 R_2^0,\\
&a_{16} = -K_{11}^0 + \frac{a_{15}}{a_6}, \quad a_{17} = -K_{12}^0 - K_{44}^0 + \frac{a_{15}}{a_6}, \quad a_{18} = -K_{11}^0 R_2^0 + K_{12}^0 R_1^0, \quad a_{19} = -C_{11}^0 K_{12}^0 + R_1^0 R_2^0,\\
&a_{20} = \frac{K_{11}^0}{a_6}, \quad a_{21} = -\frac{R_1^0}{a_6}, \quad b_1 = a_8 \frac{\partial^2}{\partial x^2} - a_2 \frac{\partial^2}{\partial y^2}, \quad b_2 = a_{16} \frac{\partial^2}{\partial x^2} - a_4 \frac{\partial^2}{\partial y^2}.
\end{aligned} \tag{A.1}
$$

State equations for SSSS

$$
\begin{aligned}
\frac{\mathrm{d}\tilde{u}_{xr}}{\mathrm{d}z} &= \frac{a_4}{a_1}\tilde{\sigma}_{xzr} - \frac{a_3}{a_1}\tilde{H}_{xzr} + \left(\frac{a_3^2 - a_2 a_4}{a_1}\right)\sum_{k=2}^{N-1} X_{rk}^{(1)} \tilde{u}_{zk} (2 \le r \le N-1),\\
\frac{\mathrm{d}\tilde{u}_{yr}}{\mathrm{d}z} &= \frac{a_4}{a_1}\tilde{\sigma}_{yzr} + \frac{a_4}{a_1}\tilde{H}_{yzr} + \left(\frac{a_3^2 - a_2 a_4}{a_1}\right) q\tilde{u}_{zr} (2 \le r \le N-1),\\
\frac{\mathrm{d}\tilde{w}_{xr}}{\mathrm{d}z} &= -\frac{a_3}{a_1}\tilde{\sigma}_{xzr} + \frac{a_2}{a_1}\tilde{H}_{xzr} + \left(\frac{a_3^2 - a_2 a_4}{a_1}\right)\sum_{k=2}^{N-1} X_{rk}^{(1)} \tilde{w}_{zk} (2 \le r \le N-1),\\
\frac{\mathrm{d}\tilde{w}_{yr}}{\mathrm{d}z} &= -\frac{a_3}{a_1}\tilde{\sigma}_{yzr} + \frac{a_2}{a_1}\tilde{H}_{yzr} + \left(\frac{a_3^2 - a_2 a_4}{a_1}\right) q\tilde{w}_{zr} (2 \le r \le N-1),\\
\frac{\mathrm{d}\tilde{\sigma}_{zzr}}{\mathrm{d}z} &= -\sum_{k=2}^{N-1} X_{rk}^{(1)} \tilde{\sigma}_{xzr} + q\tilde{\sigma}_{yzr} - a_2 \sum_{k=2}^{N-1} f_{rk}\tilde{u}_{zk} - a_3 \sum_{k=2}^{N-1} f_{rk}\tilde{w}_{zk} (2 \le r \le N-1),\\
\frac{\mathrm{d}\tilde{H}_{zzr}}{\mathrm{d}z} &= -\sum_{k=2}^{N-1} X_{rk}^{(1)} \tilde{H}_{xzr} + q\tilde{H}_{yzr} - a_3 \sum_{k=2}^{N-1} f_{rk}\tilde{u}_{zk} - a_4 \sum_{k=2}^{N-1} f_{rk}\tilde{w}_{zk} (2 \le r \le N-1),\\
\frac{\mathrm{d}\tilde{\sigma}_{xzr}}{\mathrm{d}z} &= a_8 \sum_{k=2}^{N-1} X_{rk}^{(2)} \tilde{u}_{xk} + a_2 q^2 \tilde{u}_{xr} - \frac{a_7}{a_6} \sum_{k=2}^{N-1} f_{rk}\tilde{u}_{xk} - a_9 q \sum_{k=2}^{N-1} X_{rk}^{(1)} \tilde{u}_{yk} + a_{11} \sum_{k=2}^{N-1} X_{rk}^{(2)} \tilde{w}_{xk} + a_3 q^2 \tilde{w}_{xr}\\
&\quad - \frac{a_{10}}{a_6} \sum_{k=2}^{N-1} f_{rk}\tilde{w}_{xk} - a_{12} q \sum_{k=2}^{N-1} X_{rk}^{(1)} \tilde{w}_{yk} + \frac{a_{13}}{a_6} \sum_{k=2}^{N-1} X_{rk}^{(1)} \tilde{\sigma}_{zzk} + \frac{a_{14}}{a_6} \sum_{k=2}^{N-1} X_{rk}^{(1)} \tilde{H}_{zzk} (2 \le r \le N-1),\\
\frac{\mathrm{d}\tilde{\sigma}_{yzr}}{\mathrm{d}z} &= a_9 q \sum_{k=2}^{N-1} X_{rk}^{(1)} \tilde{u}_{xk} - a_2 \sum_{k=2}^{N-1} X_{rk}^{(2)} \tilde{u}_{yk} - a_8 q^2 \tilde{u}_{yr} + a_{12} q \sum_{k=2}^{N-1} X_{rk}^{(1)} \tilde{w}_{xk}
\end{aligned}
$$

$$
\begin{aligned}
&- a_3 \sum_{k=2}^{N-1} X_{rk}^{(2)} \tilde{w}_{yk} - a_{11} q^2 \tilde{w}_{yr} + \frac{a_{13}}{a_6} q \tilde{\sigma}_{zzr} + \frac{a_{14}}{a_6} q \tilde{H}_{zzr} (2 \le r \le N-1), \\
\frac{\mathrm{d}\tilde{H}_{xzr}}{\mathrm{d}z} &= a_{11} \sum_{k=2}^{N-1} X_{rk}^{(2)} \tilde{u}_{xk} + a_3 q^2 \tilde{u}_{xr} - \frac{a_{10}}{a_6} \sum_{k=2}^{N-1} f_{rk} \tilde{u}_{xk} - a_{12} q \sum_{k=2}^{N-1} X_{rk}^{(1)} \tilde{u}_{yk} + a_{16} \sum_{k=2}^{N-1} X_{rk}^{(2)} \tilde{w}_{xk} + a_4 q^2 \tilde{w}_{xr} \\
&\quad - \frac{a_{15}}{a_6} \sum_{k=2}^{N-1} f_{rk} \tilde{w}_{xk} - a_{17} q \sum_{k=2}^{N-1} X_{rk}^{(1)} \tilde{w}_{yk} + \frac{a_{18}}{a_6} \sum_{k=2}^{N-1} X_{rk}^{(1)} \tilde{\sigma}_{zzk} + \frac{a_{19}}{a_6} \sum_{k=2}^{N-1} X_{rk}^{(1)} \tilde{H}_{zzk} (2 \le r \le N-1), \\
\frac{\mathrm{d}\tilde{H}_{yzr}}{\mathrm{d}z} &= a_{12} q \sum_{k=2}^{N-1} X_{rk}^{(1)} \tilde{u}_{xk} - a_3 \sum_{k=2}^{N-1} X_{rk}^{(2)} \tilde{u}_{yk} - a_{11} q^2 \tilde{u}_{yr} + a_{17} q \sum_{k=2}^{N-1} X_{rk}^{(1)} \tilde{w}_{xk} - a_4 \sum_{k=2}^{N-1} X_{rk}^{(2)} \tilde{w}_{yk} \\
&\quad - a_{16} q^2 \tilde{w}_{yr} + \frac{a_{18}}{a_6} q \tilde{\sigma}_{zzr} + \frac{a_{19}}{a_6} q \tilde{H}_{zzr} (2 \le r \le N-1), \\
\frac{\mathrm{d}\tilde{u}_{zr}}{\mathrm{d}z} &= \frac{a_{13}}{a_6} \sum_{k=2}^{N-1} X_{rk}^{(1)} \tilde{u}_{xk} - \frac{a_{13}}{a_6} q \tilde{u}_{yr} + \frac{a_{18}}{a_6} \sum_{k=2}^{N-1} X_{rk}^{(1)} \tilde{w}_{xk} - \frac{a_{18}}{a_6} q \tilde{w}_{yr} + a_{20} \tilde{\sigma}_{zzr} + a_{21} \tilde{H}_{zzr} (2 \le r \le N-1), \\
\frac{\mathrm{d}\tilde{w}_{zr}}{\mathrm{d}z} &= \frac{a_{14}}{a_6} \sum_{k=2}^{N-1} X_{rk}^{(1)} \tilde{u}_{xk} - \frac{a_{14}}{a_6} q \tilde{u}_{yr} + \frac{a_{19}}{a_6} \sum_{k=2}^{N-1} X_{rk}^{(1)} \tilde{w}_{xk} - \frac{a_{19}}{a_6} q \tilde{w}_{yr} + a_{21} \tilde{\sigma}_{zzr} + a_5 \tilde{H}_{zzr} (2 \le r \le N-1).
\end{aligned} \tag{A.2}
$$

State equations for CSCS

$$
\begin{aligned}
\frac{\mathrm{d}\tilde{u}_{xr}}{\mathrm{d}z} &= \frac{a_4}{a_1} \tilde{\sigma}_{xzr} - \frac{a_3}{a_1} \tilde{H}_{xzr} + \left(\frac{a_3^2 - a_2 a_4}{a_1} \right) \sum_{k=2}^{N-1} X_{rk}^{(1)} \tilde{u}_{zk} (2 \le r \le N-1), \\
\frac{\mathrm{d}\tilde{u}_{yr}}{\mathrm{d}z} &= \frac{a_4}{a_1} \tilde{\sigma}_{yzr} + \frac{a_4}{a_1} \tilde{H}_{yzr} + \left(\frac{a_3^2 - a_2 a_4}{a_1} \right) q \tilde{u}_{zr} (2 \le r \le N-1), \\
\frac{\mathrm{d}\tilde{w}_{xr}}{\mathrm{d}z} &= -\frac{a_3}{a_1} \tilde{\sigma}_{xzr} + \frac{a_2}{a_1} \tilde{H}_{xzr} + \left(\frac{a_3^2 - a_2 a_4}{a_1} \right) \sum_{k=2}^{N-1} X_{rk}^{(1)} \tilde{w}_{zk} (2 \le r \le N-1), \\
\frac{\mathrm{d}\tilde{w}_{yr}}{\mathrm{d}z} &= -\frac{a_3}{a_1} \tilde{\sigma}_{yzr} + \frac{a_2}{a_1} \tilde{H}_{yzr} + \left(\frac{a_3^2 - a_2 a_4}{a_1} \right) q \tilde{w}_{zr} (2 \le r \le N-1), \\
\frac{\mathrm{d}\tilde{\sigma}_{zzr}}{\mathrm{d}z} &= -\sum_{k=2}^{N-1} X_{rk}^{(1)} \tilde{\sigma}_{xzr} + q \tilde{\sigma}_{yzr} - a_2 \sum_{k=2}^{N-1} f_{rk} \tilde{u}_{zk} - a_3 \sum_{k=2}^{N-1} f_{rk} \tilde{w}_{zk} (2 \le r \le N-1), \\
\frac{\mathrm{d}\tilde{H}_{zzr}}{\mathrm{d}z} &= -\sum_{k=2}^{N-1} X_{rk}^{(1)} \tilde{H}_{xzr} + q \tilde{H}_{yzr} - a_3 \sum_{k=2}^{N-1} f_{rk} \tilde{u}_{zk} - a_4 \sum_{k=2}^{N-1} f_{rk} \tilde{w}_{zk} (2 \le r \le N-1), \\
\frac{\mathrm{d}\tilde{\sigma}_{xzr}}{\mathrm{d}z} &= a_8 \sum_{k=2}^{N-1} X_{rk}^{(2)} \tilde{u}_{xk} + a_2 q^2 \tilde{u}_{xr} - \frac{a_7}{a_6} \sum_{k=2}^{N-1} f_{rk} \tilde{u}_{xk} - a_9 q \sum_{k=2}^{N-1} X_{rk}^{(1)} \tilde{u}_{yk} + a_{11} \sum_{k=2}^{N-1} X_{rk}^{(2)} \tilde{w}_{xk} + a_3 q^2 \tilde{w}_{xr} \\
&\quad - \frac{a_{10}}{a_6} \sum_{k=2}^{N-1} f_{rk} \tilde{w}_{xk} - a_{12} q \sum_{k=2}^{N-1} X_{rk}^{(1)} \tilde{w}_{yk} + \frac{a_{13}}{a_6} \sum_{k=2}^{N-1} X_{rk}^{(1)} \tilde{\sigma}_{zzk} + \frac{a_{14}}{a_6} \sum_{k=2}^{N-1} X_{rk}^{(1)} \tilde{H}_{zzk} (2 \le r \le N-1), \\
\frac{\mathrm{d}\tilde{\sigma}_{yzr}}{\mathrm{d}z} &= a_9 q \sum_{k=2}^{N-1} X_{rk}^{(1)} \tilde{u}_{xk} - a_2 \sum_{k=2}^{N-1} X_{rk}^{(2)} \tilde{u}_{yk} - a_8 q^2 \tilde{u}_{yr} + a_{12} q \sum_{k=2}^{N-1} X_{rk}^{(1)} \tilde{w}_{xk} \\
&\quad - a_3 \sum_{k=2}^{N-1} X_{rk}^{(2)} \tilde{w}_{yk} - a_{11} q^2 \tilde{w}_{yr} + \frac{a_{13}}{a_6} q \tilde{\sigma}_{zzr} + \frac{a_{14}}{a_6} q \tilde{H}_{zzr} (2 \le r \le N-1),
\end{aligned}
$$

$$
\begin{aligned}
\frac{\mathrm{d}\tilde{H}_{xzr}}{\mathrm{d}z} &= a_{11}\sum_{k=2}^{N-1}X_{rk}^{(2)}\tilde{u}_{xk}+a_3q^2\tilde{u}_{xr}-\frac{a_{10}}{a_6}\sum_{k=2}^{N-1}f_{rk}\tilde{u}_{xk}-a_{12}q\sum_{k=2}^{N-1}X_{rk}^{(1)}\tilde{u}_{yk}+a_{16}\sum_{k=2}^{N-1}X_{rk}^{(2)}\tilde{w}_{xk}+a_4q^2\tilde{w}_{xr}\\
&\quad-\frac{a_{15}}{a_6}\sum_{k=2}^{N-1}f_{rk}\tilde{w}_{xk}-a_{17}q\sum_{k=2}^{N-1}X_{rk}^{(1)}\tilde{w}_{yk}+\frac{a_{18}}{a_6}\sum_{k=2}^{N-1}X_{rk}^{(1)}\tilde{\sigma}_{zzk}+\frac{a_{19}}{a_6}\sum_{k=2}^{N-1}X_{rk}^{(1)}\tilde{H}_{zzk}(2\le r\le N-1),\\
\frac{\mathrm{d}\tilde{H}_{yzr}}{\mathrm{d}z} &= a_{12}q\sum_{k=2}^{N-1}X_{rk}^{(1)}\tilde{u}_{xk}-a_3\sum_{k=2}^{N-1}X_{rk}^{(2)}\tilde{u}_{yk}-a_{11}q^2\tilde{u}_{yr}+a_{17}q\sum_{k=2}^{N-1}X_{rk}^{(1)}\tilde{w}_{xk}-a_4\sum_{k=2}^{N-1}X_{rk}^{(2)}\tilde{w}_{yk}\\
&\quad-a_{16}q^2\tilde{w}_{yr}+\frac{a_{18}}{a_6}q\tilde{\sigma}_{zzr}+\frac{a_{19}}{a_6}q\tilde{H}_{zzr}(2\le r\le N-1),\\
\frac{\mathrm{d}\tilde{u}_{zr}}{\mathrm{d}z} &= \frac{a_{13}}{a_6}\sum_{k=2}^{N-1}X_{rk}^{(1)}\tilde{u}_{xk}-\frac{a_{13}}{a_6}q\tilde{u}_{yr}+\frac{a_{18}}{a_6}\sum_{k=2}^{N-1}X_{rk}^{(1)}\tilde{w}_{xk}-\frac{a_{18}}{a_6}q\tilde{w}_{yr}+a_{20}\tilde{\sigma}_{zzr}+a_{21}\tilde{H}_{zzr}(2\le r\le N-1),\\
\frac{\mathrm{d}\tilde{w}_{zr}}{\mathrm{d}z} &= \frac{a_{14}}{a_6}\sum_{k=2}^{N-1}X_{rk}^{(1)}\tilde{u}_{xk}-\frac{a_{14}}{a_6}q\tilde{u}_{yr}+\frac{a_{19}}{a_6}\sum_{k=2}^{N-1}X_{rk}^{(1)}\tilde{w}_{xk}-\frac{a_{19}}{a_6}q\tilde{w}_{yr}+a_{21}\tilde{\sigma}_{zzr}+a_5\tilde{H}_{zzr}(2\le r\le N-1).
\end{aligned}
\tag{A.3}
$$

State equations for CSSS

$$
\begin{aligned}
\frac{\mathrm{d}\tilde{u}_{xr}}{\mathrm{d}z} &= \frac{a_4}{a_1}\tilde{\sigma}_{xzr}-\frac{a_3}{a_1}\tilde{H}_{xzr}+\left(\frac{a_3^2-a_2a_4}{a_1}\right)\sum_{k=2}^{N-1}X_{rk}^{(1)}\tilde{u}_{zk}(2\le r\le N),\\
\frac{\mathrm{d}\tilde{u}_{yr}}{\mathrm{d}z} &= \frac{a_4}{a_1}\tilde{\sigma}_{yzr}+\frac{a_4}{a_1}\tilde{H}_{yzr}+\left(\frac{a_3^2-a_2a_4}{a_1}\right)q\tilde{u}_{zr}(2\le r\le N-1),\\
\frac{\mathrm{d}\tilde{w}_{xr}}{\mathrm{d}z} &= -\frac{a_3}{a_1}\tilde{\sigma}_{xzr}+\frac{a_2}{a_1}\tilde{H}_{xzr}+\left(\frac{a_3^2-a_2a_4}{a_1}\right)\sum_{k=2}^{N-1}X_{rk}^{(1)}\tilde{w}_{zk}(2\le r\le N),\\
\frac{\mathrm{d}\tilde{w}_{yr}}{\mathrm{d}z} &= -\frac{a_3}{a_1}\tilde{\sigma}_{yzr}+\frac{a_2}{a_1}\tilde{H}_{yzr}+\left(\frac{a_3^2-a_2a_4}{a_1}\right)q\tilde{w}_{zr}(2\le r\le N-1),\\
\frac{\mathrm{d}\tilde{\sigma}_{zzr}}{\mathrm{d}z} &= -\sum_{k=2}^{N}X_{rk}^{(1)}\tilde{\sigma}_{xzr}+q\tilde{\sigma}_{yzr}-a_2\sum_{k=2}^{N-1}f_{1rk}\tilde{u}_{zk}-a_3\sum_{k=2}^{N-1}f_{1rk}\tilde{w}_{zk}(2\le r\le N-1),\\
\frac{\mathrm{d}\tilde{H}_{zzr}}{\mathrm{d}z} &= -\sum_{k=2}^{N}X_{rk}^{(1)}\tilde{H}_{xzr}+q\tilde{H}_{yzr}-a_3\sum_{k=2}^{N-1}f_{1rk}\tilde{u}_{zk}-a_4\sum_{k=2}^{N-1}f_{1rk}\tilde{w}_{zk}(2\le r\le N-1),\\
\frac{\mathrm{d}\tilde{\sigma}_{xzr}}{\mathrm{d}z} &= a_8\sum_{k=2}^{N}X_{rk}^{(2)}\tilde{u}_{xk}+a_2q^2\tilde{u}_{xr}-\frac{a_7}{a_6}\sum_{k=2}^{N}f_{1rk}\tilde{u}_{xk}-a_8\sum_{k=2}^{N}f_{Nrk}\tilde{u}_{xk}-a_9q\sum_{k=2}^{N-1}X_{rk}^{(1)}\tilde{u}_{yk}\\
&\quad+a_{11}\sum_{k=2}^{N}X_{rk}^{(2)}\tilde{w}_{xk}+a_3q^2\tilde{w}_{xr}-\frac{a_{10}}{a_6}\sum_{k=2}^{N}f_{1rk}\tilde{w}_{xk}-a_{11}\sum_{k=2}^{N}f_{Nrk}\tilde{w}_{xk}-a_{12}q\sum_{k=2}^{N-1}X_{rk}^{(1)}\tilde{w}_{yk}\\
&\quad+\frac{a_{13}}{a_6}\sum_{k=2}^{N-1}X_{rk}^{(1)}\tilde{\sigma}_{zzk}+\frac{a_{14}}{a_6}\sum_{k=2}^{N-1}X_{rk}^{(1)}\tilde{H}_{zzk}(2\le r\le N),\\
\frac{\mathrm{d}\tilde{\sigma}_{yzr}}{\mathrm{d}z} &= a_9q\sum_{k=2}^{N}X_{rk}^{(1)}\tilde{u}_{xk}-a_2\sum_{k=2}^{N-1}X_{rk}^{(2)}\tilde{u}_{yk}-a_8q^2\tilde{u}_{yr}+a_{12}q\sum_{k=2}^{N}X_{rk}^{(1)}\tilde{w}_{xk}\\
&\quad-a_3\sum_{k=2}^{N-1}X_{rk}^{(2)}\tilde{w}_{yk}-a_{11}q^2\tilde{w}_{yr}+\frac{a_{13}}{a_6}q\tilde{\sigma}_{zzr}+\frac{a_{14}}{a_6}q\tilde{H}_{zzr}(2\le r\le N-1),
\end{aligned}
$$

$$\begin{aligned}
\frac{\mathrm{d}\tilde{H}_{xzr}}{\mathrm{d}z} &= a_{11}\sum_{k=2}^{N} X_{rk}^{(2)}\tilde{u}_{xk} + a_3 q^2\tilde{u}_{xr} - \frac{a_{10}}{a_6}\sum_{k=2}^{N} f_{1rk}\tilde{u}_{xk} - a_{11}\sum_{k=2}^{N} f_{Nrk}\tilde{u}_{xk} - a_{12}q\sum_{k=2}^{N-1} X_{rk}^{(1)}\tilde{u}_{yk} + a_{16}\sum_{k=2}^{N} X_{rk}^{(2)}\tilde{w}_{xk} \\
&\quad + a_4 q^2\tilde{w}_{xr} - \frac{a_{15}}{a_6}\sum_{k=2}^{N} f_{1rk}\tilde{w}_{xk} - a_{16}\sum_{k=2}^{N} f_{Nrk}\tilde{w}_{xk} - a_{17}q\sum_{k=2}^{N-1} X_{rk}^{(1)}\tilde{w}_{yk} + \frac{a_{18}}{a_6}\sum_{k=2}^{N-1} X_{rk}^{(1)}\tilde{\sigma}_{zzk} \\
&\quad + \frac{a_{19}}{a_6}\sum_{k=2}^{N-1} X_{rk}^{(1)}\tilde{H}_{zzk} (2 \le r \le N), \\
\frac{\mathrm{d}\tilde{H}_{yzr}}{\mathrm{d}z} &= a_{12}q\sum_{k=2}^{N} X_{rk}^{(1)}\tilde{u}_{xk} - a_3\sum_{k=2}^{N-1} X_{rk}^{(2)}\tilde{u}_{yk} - a_{11}q^2\tilde{u}_{yr} + a_{17}q\sum_{k=2}^{N} X_{rk}^{(1)}\tilde{w}_{xk} - a_4\sum_{k=2}^{N-1} X_{rk}^{(2)}\tilde{w}_{yk} \\
&\quad - a_{16}q^2\tilde{w}_{yr} + \frac{a_{18}}{a_6}q\tilde{\sigma}_{zzr} + \frac{a_{19}}{a_6}q\tilde{H}_{zzr} (2 \le r \le N-1), \\
\frac{\mathrm{d}\tilde{u}_{zr}}{\mathrm{d}z} &= \frac{a_{13}}{a_6}\sum_{k=2}^{N} X_{rk}^{(1)}\tilde{u}_{xk} - \frac{a_{13}}{a_6}q\tilde{u}_{yr} + \frac{a_{18}}{a_6}\sum_{k=2}^{N} X_{rk}^{(1)}\tilde{w}_{xk} - \frac{a_{18}}{a_6}q\tilde{w}_{yr} + a_{20}\tilde{\sigma}_{zzr} + a_{21}\tilde{H}_{zzr} (2 \le r \le N-1), \\
\frac{\mathrm{d}\tilde{w}_{zr}}{\mathrm{d}z} &= \frac{a_{14}}{a_6}\sum_{k=2}^{N} X_{rk}^{(1)}\tilde{u}_{xk} - \frac{a_{14}}{a_6}q\tilde{u}_{yr} + \frac{a_{19}}{a_6}\sum_{k=2}^{N} X_{rk}^{(1)}\tilde{w}_{xk} - \frac{a_{19}}{a_6}q\tilde{w}_{yr} + a_{21}\tilde{\sigma}_{zzr} + a_5\tilde{H}_{zzr} (2 \le r \le N-1), \quad \text{(A.4)}
\end{aligned}$$

with $f_{1rk} = X_{r1}^{(1)}X_{1k}^{(1)},\ f_{Nrk} = X_{rN}^{(1)}X_{Nr}^{(1)},\ f_{rk} = f_{1rk} + f_{Nrk}$.

State equations for CSFS

$$\begin{aligned}
\frac{\mathrm{d}\tilde{u}_{xr}}{\mathrm{d}z} &= \frac{a_4}{a_1}\tilde{\sigma}_{xzr} - \frac{a_3}{a_1}\tilde{H}_{xzr} + \left(\frac{a_3^2 - a_2a_4}{a_1}\right)\sum_{k=2}^{N} X_{rk}^{(1)}\tilde{u}_{zk} (2 \le r \le N-1), \\
\frac{\mathrm{d}\tilde{u}_{yr}}{\mathrm{d}z} &= \frac{a_4}{a_1}\tilde{\sigma}_{yzr} + \frac{a_4}{a_1}\tilde{H}_{yzr} + \left(\frac{a_3^2 - a_2a_4}{a_1}\right)q\tilde{u}_{zr} (2 \le r \le N), \\
\frac{\mathrm{d}\tilde{w}_{xr}}{\mathrm{d}z} &= -\frac{a_3}{a_1}\tilde{\sigma}_{xzr} + \frac{a_2}{a_1}\tilde{H}_{xzr} + \left(\frac{a_3^2 - a_2a_4}{a_1}\right)\sum_{k=2}^{N} X_{rk}^{(1)}\tilde{w}_{zk} (2 \le r \le N-1), \\
\frac{\mathrm{d}\tilde{w}_{yr}}{\mathrm{d}z} &= -\frac{a_3}{a_1}\tilde{\sigma}_{yzr} + \frac{a_2}{a_1}\tilde{H}_{yzr} + \left(\frac{a_3^2 - a_2a_4}{a_1}\right)q\tilde{w}_{zr} (2 \le r \le N), \\
\frac{\mathrm{d}\tilde{\sigma}_{zzr}}{\mathrm{d}z} &= -\sum_{k=2}^{N-1} X_{rk}^{(1)}\tilde{\sigma}_{xzr} + q\mathbf{E}_1\tilde{\sigma}_{yzr} - a_2\sum_{k=2}^{N} f_{1rk}\tilde{u}_{zk} - a_3\sum_{k=2}^{N} f_{1rk}\tilde{w}_{zk} (1 \le r \le N-1), \\
\frac{\mathrm{d}\tilde{H}_{zzr}}{\mathrm{d}z} &= -\sum_{k=2}^{N-1} X_{rk}^{(1)}\tilde{H}_{xzr} + q\mathbf{E}_1\tilde{H}_{yzr} - a_3\sum_{k=2}^{N} f_{1rk}\tilde{u}_{zk} - a_4\sum_{k=2}^{N} f_{1rk}\tilde{w}_{zk} (1 \le r \le N-1), \\
\frac{\mathrm{d}\tilde{\sigma}_{xzr}}{\mathrm{d}z} &= a_8\sum_{k=2}^{N-1} X_{rk}^{(2)}\tilde{u}_{xk} + a_2q^2\tilde{u}_{xr} - \frac{a_7}{a_6}\sum_{k=2}^{N-1} f_{1rk}\tilde{u}_{xk} - \left(\frac{a_{13}c_2}{a_6c_1} + \frac{a_{14}c_4}{a_6c_1}\right)\sum_{k=2}^{N-1} f_{Nrk}\tilde{u}_{xk} - a_9q\sum_{k=2}^{N} X_{rk}^{(1)}\tilde{u}_{yk} \\
&\quad + \left(\frac{a_{13}c_3}{a_6} + \frac{a_{14}c_5}{a_6}\right)q\mathbf{E}_6\tilde{u}_{yr} - \frac{a_8}{q}\sum_{k=2}^{N} F_{Nrk}\tilde{u}_{yk} + \frac{a_7}{a_6q}\sum_{k=2}^{N}\overline{F}_{Nrk}\tilde{u}_{yk} + \left(\frac{a_{13}c_2}{a_6c_1} + \frac{a_{14}c_4}{a_6c_1}\right)\frac{1}{q}\sum_{k=2}^{N}\overline{\overline{F}}_{Nrk}\tilde{u}_{yk} \\
&\quad + a_{11}\sum_{k=2}^{N-1} X_{rk}^{(2)}\tilde{w}_{xk} + a_3q^2\tilde{w}_{xr} - \frac{a_{10}}{a_6}\sum_{k=2}^{N-1} f_{1rk}\tilde{w}_{xk} - \left(\frac{a_{13}c_4}{a_6c_1} + \frac{a_{14}c_6}{a_6c_1}\right)\sum_{k=2}^{N-1} f_{Nrk}\tilde{w}_{xk} - a_{12}q\sum_{k=2}^{N} X_{rk}^{(1)}\tilde{w}_{yk} \\
&\quad + \left(\frac{a_{13}c_5}{a_6} + \frac{a_{14}c_7}{a_6}\right)q\mathbf{E}_6\tilde{w}_{yr} - \frac{a_{11}}{q}\sum_{k=2}^{N} F_{Nrk}\tilde{w}_{yk} + \frac{a_{10}}{a_6q}\sum_{k=2}^{N}\overline{F}_{Nrk}\tilde{w}_{yk} + \left(\frac{a_{13}c_4}{a_6c_1} + \frac{a_{14}c_6}{a_6c_1}\right)\frac{1}{q}\sum_{k=2}^{N}\overline{\overline{F}}_{Nrk}\tilde{w}_{yk} \\
&\quad + \frac{a_{13}}{a_6}\sum_{k=2}^{N} X_{rk}^{(1)}\tilde{\sigma}_{zzk} + \frac{a_{14}}{a_6}\sum_{k=2}^{N} X_{rk}^{(1)}\tilde{H}_{zzk} (2 \le r \le N-1), \quad \text{(A5)}
\end{aligned}$$

$$
\begin{aligned}
\frac{\mathrm{d}\tilde{\sigma}_{yzr}}{\mathrm{d}z} &= a_9 q \sum_{k=2}^{N-1} X_{rk}^{(1)} \tilde{u}_{xk} - \left(\frac{a_{13}c_2}{a_6c_1} + \frac{a_{14}c_4}{a_6c_1}\right) q\mathbf{E}_4 \tilde{u}_{xr} - a_2 \sum_{k=2}^{N} X_{rk}^{(2)} \tilde{u}_{yk} - a_8 q^2 \tilde{u}_{yr} + (\frac{a_{13}c_3}{a_6c_1} + \frac{a_{14}c_5}{a_6c_1}) q^2 \mathbf{E}_3 \tilde{u}_{yr} \\
&\quad - a_9 \sum_{k=2}^{N} f_{Nrk} \tilde{u}_{yk} + \left(\frac{a_{13}c_2}{a_6c_1} + \frac{a_{14}c_4}{a_6c_1}\right) \mathbf{E}_5 \tilde{u}_{yr} + a_{12} q \sum_{k=2}^{N-1} X_{rk}^{(1)} \tilde{w}_{xk} - \left(\frac{a_{13}c_4}{a_6c_1} + \frac{a_{14}c_6}{a_6c_1}\right) q\mathbf{E}_4 \tilde{w}_{xr} \\
&\quad - a_3 \sum_{k=2}^{N} X_{rk}^{(2)} \tilde{w}_{yk} - a_{11} q^2 \tilde{w}_{yr} + \left(\frac{a_{13}c_5}{a_6c_1} + \frac{a_{14}c_7}{a_6c_1}\right) q^2 \mathbf{E}_3 \tilde{w}_{yr} - a_{12} \sum_{k=2}^{N} f_{Nrk} \tilde{w}_{yk} + \left(\frac{a_{13}c_4}{a_6c_1} + \frac{a_{14}c_6}{a_6c_1}\right) \mathbf{E}_5 \tilde{w}_{yr} \\
&\quad + \frac{a_{13}}{a_6} q\mathbf{E}_2 \tilde{\sigma}_{zzr} + \frac{a_{14}}{a_6} q\mathbf{E}_2 \tilde{H}_{zzr} (2 \le r \le N), \\
\frac{\mathrm{d}\tilde{H}_{xzr}}{\mathrm{d}z} &= a_{11} \sum_{k=2}^{N-1} X_{rk}^{(2)} \tilde{u}_{xk} + a_3 q^2 \tilde{u}_{xr} - \frac{a_{10}}{a_6} \sum_{k=2}^{N-1} f_{1rk} \tilde{u}_{xk} - \left(\frac{a_{18}c_2}{a_6c_1} + \frac{a_{19}c_4}{a_6c_1}\right) \sum_{k=2}^{N-1} f_{Nrk} \tilde{u}_{xk} - a_{12} q \sum_{k=2}^{N} X_{rk}^{(1)} \tilde{u}_{yk} \\
&\quad + \left(\frac{a_{18}c_3}{a_6} + \frac{a_{19}c_5}{a_6}\right) q\mathbf{E}_6 \tilde{u}_{yr} - \frac{a_{11}}{q} \sum_{k=2}^{N} F_{Nrk} \tilde{u}_{yk} + \frac{a_{10}}{a_6 q} \sum_{k=2}^{N} \overline{F}_{Nrk} \tilde{u}_{yk} + \left(\frac{a_{18}c_2}{a_6c_1} + \frac{a_{19}c_4}{a_6c_1}\right) \frac{1}{q} \sum_{k=2}^{N} \overline{\overline{F}}_{Nrk} \tilde{u}_{yk} \\
&\quad + a_{16} \sum_{k=2}^{N-1} X_{rk}^{(2)} \tilde{w}_{xk} + a_4 q^2 \tilde{w}_{xr} - \frac{a_{15}}{a_6} \sum_{k=2}^{N-1} f_{1rk} \tilde{w}_{xk} - \left(\frac{a_{18}c_4}{a_6c_1} + \frac{a_{19}c_6}{a_6c_1}\right) \sum_{k=2}^{N-1} f_{Nrk} \tilde{w}_{xk} - a_{17} q \sum_{k=2}^{N} X_{rk}^{(1)} \tilde{w}_{yk} \\
&\quad + \left(\frac{a_{18}c_5}{a_6} + \frac{a_{19}c_7}{a_6}\right) q\mathbf{E}_6 \tilde{w}_{yr} - \frac{a_{16}}{q} \sum_{k=2}^{N} F_{Nrk} \tilde{w}_{yk} + \frac{a_{15}}{a_6 q} \sum_{k=2}^{N} \overline{F}_{Nrk} \tilde{w}_{yk} + \left(\frac{a_{18}c_4}{a_6c_1} + \frac{a_{19}c_6}{a_6c_1}\right) \frac{1}{q} \sum_{k=2}^{N} \overline{\overline{F}}_{Nrk} \tilde{w}_{yk} \\
&\quad + \frac{a_{18}}{a_6} \sum_{k=1}^{N-1} X_{rk}^{(1)} \tilde{\sigma}_{zzk} + \frac{a_{19}}{a_6} \sum_{k=1}^{N-1} X_{rk}^{(1)} \tilde{H}_{zzk} (2 \le r \le N-1),
\end{aligned}
$$

$$
\begin{aligned}
\frac{\mathrm{d}\tilde{H}_{yzr}}{\mathrm{d}z} &= a_{12} q \sum_{k=2}^{N-1} X_{rk}^{(1)} \tilde{u}_{xk} - \left(\frac{a_{18}c_2}{a_6c_1} + \frac{a_{19}c_4}{a_6c_1}\right) q\mathbf{E}_4 \tilde{u}_{xr} - a_3 \sum_{k=2}^{N} X_{rk}^{(2)} \tilde{u}_{yk} - a_{11} q^2 \tilde{u}_{yr} + \left(\frac{a_{18}c_3}{a_6c_1} + \frac{a_{19}c_5}{a_6c_1}\right) q^2 \mathbf{E}_3 \tilde{u}_{yr} \\
&\quad - a_{12} \sum_{k=2}^{N} f_{Nrk} \tilde{u}_{yk} + \left(\frac{a_{18}c_2}{a_6c_1} + \frac{a_{19}c_4}{a_6c_1}\right) \mathbf{E}_5 \tilde{u}_{yr} + a_{17} q \sum_{k=2}^{N-1} X_{rk}^{(1)} \tilde{w}_{xk} - \left(\frac{a_{18}c_4}{a_6c_1} + \frac{a_{19}c_6}{a_6c_1}\right) q\mathbf{E}_4 \tilde{w}_{xr} \\
&\quad - a_4 \sum_{k=2}^{N} X_{rk}^{(2)} \tilde{w}_{yk} - a_{16} q^2 \tilde{w}_{yr} + \left(\frac{a_{18}c_5}{a_6c_1} + \frac{a_{19}c_7}{a_6c_1}\right) q^2 \mathbf{E}_3 \tilde{w}_{yr} - a_{17} \sum_{k=2}^{N} f_{Nrk} \tilde{w}_{yk} \\
&\quad + \left(\frac{a_{18}c_4}{a_6c_1} + \frac{a_{19}c_6}{a_6c_1}\right) \mathbf{E}_5 \tilde{w}_{yr} + \frac{a_{18}}{a_6} q\mathbf{E}_2 \tilde{\sigma}_{zzr} + \frac{a_{19}}{a_6} q\mathbf{E}_2 \tilde{H}_{zzr} (2 \le r \le N), \\
\frac{\mathrm{d}\tilde{u}_{zr}}{\mathrm{d}z} &= \frac{a_{13}}{a_6} \sum_{k=2}^{N-1} X_{rk}^{(1)} \tilde{u}_{xk} - \left(\frac{a_{20}c_2}{a_6c_1} + \frac{a_{21}c_4}{a_6c_1}\right) \mathbf{E}_4 \tilde{u}_{xr} - \frac{a_{13}}{a_6} q \tilde{u}_{yr} + \left(\frac{a_{20}c_3}{a_6c_1} + \frac{a_{21}c_5}{a_6c_1}\right) q\mathbf{E}_3 \tilde{u}_{yr} - \frac{a_{13}}{a_6 q} \sum_{k=2}^{N} f_{Nrk} \tilde{u}_{yk} \\
&\quad + \left(\frac{a_{18}c_2}{a_6c_1} + \frac{a_{21}c_4}{a_6c_1}\right) \frac{1}{q} \mathbf{E}_5 \tilde{u}_{yr} + \frac{a_{18}}{a_6} \sum_{k=2}^{N-1} X_{rk}^{(1)} \tilde{w}_{xk} - \left(\frac{a_{20}c_4}{a_6c_1} + \frac{a_{21}c_6}{a_6c_1}\right) \mathbf{E}_4 \tilde{w}_{xr} - \frac{a_{18}}{a_6} q \tilde{w}_{yr} \\
&\quad + \left(\frac{a_{20}c_5}{a_6c_1} + \frac{a_{21}c_7}{a_6c_1}\right) q\mathbf{E}_3 \tilde{w}_{yr} - \frac{a_{18}}{a_6 q} \sum_{k=2}^{N} f_{Nrk} \tilde{w}_{yk} + \left(\frac{a_{20}c_4}{a_6c_1} + \frac{a_{21}c_6}{a_6c_1}\right) \frac{1}{q} \mathbf{E}_5 \tilde{w}_{yr} \\
&\quad + a_{20} \mathbf{E}_2 \tilde{\sigma}_{zzr} + a_{21} \mathbf{E}_2 \tilde{H}_{zzr} (2 \le r \le N), \\
\frac{\mathrm{d}\tilde{w}_{zr}}{\mathrm{d}z} &= \frac{a_{14}}{a_6} \sum_{k=2}^{N-1} X_{rk}^{(1)} \tilde{u}_{xk} - \left(\frac{a_{21}c_2}{a_6c_1} + \frac{a_5c_4}{a_6c_1}\right) \mathbf{E}_4 \tilde{u}_{xr} - \frac{a_{14}}{a_6} q \tilde{u}_{yr} + \left(\frac{a_{21}c_3}{a_6c_1} + \frac{a_5c_5}{a_6c_1}\right) q\mathbf{E}_3 \tilde{u}_{yr} \\
&\quad - \frac{a_{14}}{a_6 q} \sum_{k=2}^{N} f_{Nrk} \tilde{u}_{yk} + \left(\frac{a_{21}c_2}{a_6c_1} + \frac{a_5c_4}{a_6c_1}\right) \frac{1}{q} \mathbf{E}_5 \tilde{u}_{yr} + \frac{a_{19}}{a_6} \sum_{k=2}^{N-1} X_{rk}^{(1)} \tilde{w}_{xk} - \left(\frac{a_{21}c_4}{a_6c_1} + \frac{a_5c_6}{a_6c_1}\right) \mathbf{E}_4 \tilde{w}_{xr}
\end{aligned}
$$

$$-\frac{a_{19}}{a_6}q\tilde{w}_{yr}+\left(\frac{a_{21}c_5}{a_6c_1}+\frac{a_5c_7}{a_6c_1}\right)q\mathbf{E}_3\tilde{w}_{yr}-\frac{a_{18}}{a_6q}\sum_{k=2}^{N}f_{Nrk}\tilde{w}_{yk}+\left(\frac{a_{21}c_4}{a_6c_1}+\frac{a_5c_6}{a_6c_1}\right)\frac{1}{q}\mathbf{E}_5\tilde{w}_{yr}$$
$$+a_{21}\mathbf{E}_2\tilde{\sigma}_{zzr}+a_5\mathbf{E}_2\tilde{H}_{zzr}(2\le r\le N),$$

where

$$c_1=C_{12}^0K_{12}^0-R_2^0R_2^0,\ c_2=C_{11}^0C_{11}^0K_{12}^0-2C_{11}^0R_1^0R_2^0-C_{12}^0(c_1+R_1^0R_1^0),\ c_3=C_{11}^0-C_{12}^0,$$
$$c_4=C_{11}^0R_1^0K_{12}^0+C_{12}^0R_1^0K_{11}^0-C_{11}^0R_2^0K_{11}^0-C_{12}^0R_2^0K_{12}^0-R_1^0R_1^0R_2^0+R_2^0R_2^0R_2^0,\ c_5=R_1^0-R_2^0,$$
$$c_6=C_{12}^0(K_{11}^0-K_{12}^0)(K_{11}^0+K_{12}^0)-2R_1^0R_2^0K_{11}^0+(R_1^0R_1^0+R_2^0R_2^0)K_{12}^0,\ c_7=K_{11}^0-K_{12}^0, \tag{A6}$$

$$\mathbf{E}_1=\begin{bmatrix}\mathbf{0} & 0\\ \mathbf{I}_{(N-2)\times(N-2)} & \mathbf{0}\end{bmatrix},\ \mathbf{E}_2=\begin{bmatrix}\mathbf{0} & \mathbf{I}_{(N-2)\times(N-2)}\\ 0 & \mathbf{0}\end{bmatrix},\ \mathbf{E}_3=\begin{bmatrix}\mathbf{0}_{(N-2)\times(N-2)} & \mathbf{0}\\ \mathbf{0} & 1\end{bmatrix},$$
$$\mathbf{E}_4=\begin{bmatrix}0 & \cdots & 0\\ \vdots & \ddots & \vdots\\ 0 & \cdots & 0\\ X_{N2}^{(1)} & \cdots & X_{N(N-1)}^{(1)}\end{bmatrix},\ \mathbf{E}_5=\begin{bmatrix}0 & \cdots & 0\\ \vdots & \ddots & \vdots\\ 0 & \cdots & 0\\ X_{NN}^{(1)}X_{N2}^{(1)} & \cdots & X_{NN}^{(1)}X_{NN}^{(1)}\end{bmatrix},$$
$$\mathbf{E}_6=\begin{bmatrix}0\cdots 0 & X_{N2}^{(1)}\\ \vdots\ \ddots\ \vdots & \vdots\\ 0\cdots 0 & X_{N(N-1)}^{(1)}\end{bmatrix}, \tag{A7}$$

with $F_{Nrk}=X_{rN}^{(2)}X_{kN}^{(1)}$, $\overline{F}_{Nrk}=f_{1rN}X_{kN}^{(1)}$, $\overline{\overline{F}}_{Nrk}=f_{NrN}X_{kN}^{(1)}$.

References

1. Fan, T.Y.: Mathematical Theory of Elasticity of Quasicrystals and its Applications. Springer, Heidelberg (2011)
2. Zhao, M.H., Fan, C.Y., Lu, C.S., et al.: Analysis of interface cracks in one-dimensional hexagonal quasi-crystal coating under in-plane loads. Eng. Fract. Mech. **243**(12), 107534 (2021)
3. Li, L.H., Yun, G.H.: Elastic fields around a nanosized elliptic hole in decagonal quasicrystals. Chin. Phys. B **23**(10), 106104 (2014)
4. Li, L.H., Liu, G.T.: Study on a straight dislocation in an icosahedral quasicrystal with piezoelectric effects. Appl. Math. Mech. Engl. Ed. **39**(9), 1259–1266 (2018)
5. Huang, Y.Z., Chen, J., Zhao, M., et al.: Electromechanical coupling characteristics of double-layer piezoelectric quasicrystal actuators. Int. J. Mech. Sci. **196**, 106293 (2021)
6. Pan, E.: Exact solution for functionally graded anisotropic elastic composite laminates. J. Compos. Mater. **37**(21), 1903–1920 (2003)
7. Pan, E., Han, F.: Exact solution for functionally graded and layered magneto-electro-elastic plates. Int. J. Eng. Sci. **43**(3–4), 321–339 (2005)
8. Varga, B., Fazakas, E., Varga, L.K.: Analysis of quasicrystal generation in conventionally solidified Al-Cu-Fe alloys. Met. Int. **17**(8), 27–30 (2012)
9. Ferreira, T., Koga, G.Y., De Oliveira, I.L., et al.: Functionally graded aluminum reinforced with quasicrystal approximant phases—improving the wear resistance at high temperatures. Wear **462**, 203507 (2020)
10. Ferreira, T., De Oliveira, I.L., Zepon, G., et al.: Rotational outward solidification casting: an innovative single step process to produce a functionally graded aluminum reinforced with quasicrystal approximant phases. Mater. Des. **189**, 108544 (2020)
11. Zhang, L., Guo, J.H., Xing, Y.M.: Bending deformation of multilayered one-dimensional hexagonal piezoelectric quasicrystal nanoplates with nonlocal effect. Int. J. Solids Struct. **132**, 278–302 (2018)
12. Zhang, L., Guo, J.H., Xing, Y.M.: Nonlocal analytical solution of functionally graded multilayered one-dimensional hexagonal piezoelectric quasicrystal nanoplates. Acta Mech. **230**(5), 1781–1810 (2019)
13. Huang, Y.Z., Li, Y., Yang, L.Z., et al.: Static response of functionally graded multilayered one-dimensional hexagonal piezoelectric quasicrystal plates using the state vector approach. J. Zhejiang Univ. Sci. A **20**(2), 133–147 (2019)
14. Li, Y., Yang, L.Z., Gao, Y.: Thermo-elastic analysis of functionally graded multilayered two-dimensional decagonal quasicrystal plates. ZAMM-Zeitschrift für Angewandte Mathematik und Mechanik **98**(9), 1585–1602 (2018)
15. Li, Y., Yang, L.Z., Gao, Y.: Bending analysis of laminated two-dimensional piezoelectric quasicrystal plates with functionally graded material properties. Acta Phys. Pol., A **135**(3), 426–433 (2019)
16. Mishra, S.K.: Finite element analysis of composite laminates. Sci. Rep. **4**(1), 50–50 (2012)
17. Wright, L., Robinson, S.P., Humphrey, V.F.: Prediction of acoustic radiation from axisymmetric surfaces with arbitrary boundary conditions using the boundary element method on a distributed computing system. J. Acoust. Soc. Am. **125**(3), 1374–1383 (2009)

18. Lü, C.F., Chen, W.Q., Shao, J.W.: Semi-analytical three-dimensional elasticity solutions for generally laminated composite plates. Eur. J. Mech. A-Solids **27**(5), 899–917 (2008)
19. Wang, X.W.: Differential quadrature in the analysis of structural components. Adv. Mech. **25**(2), 232–240 (1995)
20. Bellman, R., Kashef, B.G., Casti, J.: Differential quadrature: a technique for the rapid solution of nonlinear partial differential equations. J. Comput. Phys. **10**(1), 40–52 (1972)
21. Zhou, Y.Y., Chen, W.Q., Lü, C.F., et al.: Free vibration of cross-ply piezoelectric laminates in cylindrical bending with arbitrary edges. Compos. Struct. **87**(1), 93–100 (2009)
22. Zhou, Y.Y., Chen, W.Q., Lü, C.F.: Semi-analytical solution for orthotropic piezoelectric laminates in cylindrical bending with interfacial imperfections. Compos. Struct. **92**(4), 1009–1018 (2010)
23. Kamali, F., Shahabian, F.: Analytical solutions for surface stress effects on buckling and post-buckling behavior of thin symmetric porous nano-plates resting on elastic foundation. Arch. Appl. Mech. **91**(6), 2853–2880 (2021)
24. Chilton, D.S., Wekezer, J.W.: Plates on elastic foundation. J. Struct. Eng. **116**(11), 3236–3241 (1992)
25. Yas, M.H., Jodaei, A., Irandoust, S., et al.: Three-dimensional free vibration analysis of functionally graded piezoelectric annular plates on elastic foundations. Meccanica **47**(6), 1401–1423 (2011)
26. Yas, M.H., Moloudi, N.: Three-dimensional free vibration analysis of multi-directional functionally graded piezoelectric annular plates on elastic foundations via state space based differential quadrature method. Appl. Math. Mech. Engl. Ed. **36**(4), 439–464 (2015)
27. Malekzadeh, P.: Three-dimensional free vibration analysis of thick functionally graded plates on elastic foundations. Compos. Struct. **89**(3), 367–373 (2009)
28. Çerdik, Y.H.: Deriving fundamental solutions for equations of elastodynamics in three-dimensional cubic quasicrystals. Acta Phys. Pol. A **136**(3), 474–478 (2019)
29. Feng, X., Fan, X.Y., Li, Y., et al.: Static response and free vibration analysis for cubic quasicrystal laminates with imperfect interfaces. Eur. J. Mech. A. Solids **90**(14), 104365 (2021)
30. Hu, C.Z., Wang, R.H., Ding, D.H.: Symmetry groups, physical property tensors, elasticity and dislocations in quasicrystals. Rep. Prog. Phys. **63**(1), 1–39 (2000)
31. Li, Y., Yang, L.Z., Zhang, L.L., et al.: Nonlocal free and forced vibration of multilayered two-dimensional quasicrystal nanoplates. Mech. Adv. Mater. Struct. **28**(12), 1216–1226 (2021)
32. Shu, C.: Differential Quadrature and Its Application in Engineering. Springer, London (2000)
33. Bert, C.W., Malik, M.: Differential quadrature method in computational mechanics: a review. Appl. Mech. Rev. **49**(1), 1–28 (1996)
34. Hu, C.Z., Wang, R.H., Ding, D.H., et al.: Piezoelectric effects in quasicrystals. Phys. Rev. B **56**(5), 2463–2468 (1997)